1978

High shear viscometry of high polymer solutions.

Paul Li Horng
University of Massachusetts Amherst

Horng, Paul Li, "High shear viscometry of high polymer solutions." (1978). *Masters Theses 1911 - February 2014*. 1623.
Retrieved from https://scholarworks.umass.edu/theses/1623

HIGH SHEAR VISCOMETRY OF

HIGH POLYMER SOLUTIONS

A Thesis Presented

by

PAUL LI HORNG

Submitted to the Graduate School of the
University of Massachusetts in partial
fulfillment of the requirements for the degree of

MASTER OF SCIENCE

September, 1978

Polymer Science & Engineering

HIGH SHEAR VISCOMETRY OF

HIGH POLYMER SOLUTIONS

A Thesis Presented
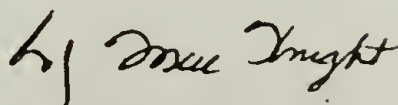
by

PAUL LI HORNG

Approved as to style and content by:

_____
Roger S. Porter
Professor of Polymer Science and Engineering
Thesis Supervisor

_____
W. J. MacKnight, Head
Polymer Science & Engineering

September, 1978

DEDICATION

To my parents and Lily

for their constant prayers,

love, and encouragement.

TABLE OF CONTENTS

ACKNOWLEDGEMENT

LIST OF TABLES

LIST OF FIGURES

C H A P T E R I

INTRODUCTION

When polymers are exposed to high shear, major deformations of the chains may be expected. The extent of deformation is a function of chain length, intermolecular interaction, shear field, temperature, and the nature and concentration of solvent. For the undiluted polymer, melt viscosities have received much attention due to its importance in processing. On the other hand, solution viscosity is a necessary tool on understanding of molecular rheology. The viscosity normally approaches a constant value, n_o, at low shear rates. When shear rate is increased, the viscosity decreases from n_o and becomes a decreasing function of shear rate. In most cases, an approximate power law dependence of viscosity at high shear rates is attained. This reversible behavior is also true for concentrated polymer solutions. Graessley[1] has developed a theory, called "chain entanglement concept", based on Rouse's bead-and-spring model for polymer rheology. This theory fits most data well on melt and concentrated solutions[1]. However, at very high shear or in low concentrations, observed viscosity[3,39,40] shows a distinct deviation from the predicted value from entanglement. This study utilizes the unique capabilities of the High Shear Viscometer and the use of series of high molecular weight polymers in low concentrations.

It is also likely that when elastic energy stored by shear input exceeds the bond energy, degradation as a result of mechanical bond

1

rupture will take place. A review on the subject of mechanochemistry by Casale, Porter and Johnson[4] indicates that numerous variables associated with degradation processes and conditions have made the comparison of results difficult. In this study, the material is subjected to a homogeneous, simple shear field with a negligible temperature variation during the shear. A permanent viscosity loss, further confirmed by molecular weight decrease, is also observed and related to the shear stress at which polymer degradation is at steady state.

CHAPTER II

EXPERIMENTS

II.A. Polymers

The polymers under investigation are solutions of atactic poly-
styrene and polyisobutene, both in decalin. Polystyrene samples are
supplied by Pressure Chemical Co., Pittsburgh, PA. and Duke Scientific
Corporation, Palo Alto, CA. Polyisobutene samples are the Vistanex
Series manufactured by Exxon (Enjay) Chemical Co., New York, N.Y.
Data on both polymers as measured by calibrated Gel Permeation Chrom-
atograph (GPC) are shown in Table I. Purified decalin solvent is ob-
tained from Fisher Scientific Co., Fairlawn, N.J. It has cis to
trans ratio of 45 to 55 from density measurement[47]. Standard oils
used to calibrate the High Shear Viscometer are specified in Table II.

Samples are prepared at room temperature to a chosen concentration
by dissolving weighed polymer into aliquot amount of solvent in glass
bottles. The bottles are only allowed to turn over twice a day and
are not agitated to avoid any possible mechanical degradation due to
use of ultra-high molecular weights. It takes seven to thirty days
for the mixtures to become homogeneous solutions. Subsequent GPC
analysis shows the materials were not degraded during the sample prep-
aration process. A comparison of columns titled "Sample" and
"Solution" in Tables III and IV shows that the variation is less than
2%.

3

II.B. High Shear Viscometer

This instrument is basically a concentric cylinder rotational couette viscometer. It was first designed by Barber[5] and was then modified and used extensively by Porter[6]. The High Shear Viscometer used in this study is the second design of this instrument[7].

The possible sources of error encountered in couette flow are minimized by the equipment design features. The test fluid is suspended by surface tension in a thin gap between cylinders. The extension of the inner rotating spindle above and below the ends of the outer cylinder eliminates end effects. The thin gap virtually guarantees a homogeneous shear field and laminar flow in the test film.

The spindles are mounted to the drive with the choice of the drive shaft of the smallest diameter, 1/8 inch, and suitable collets and chucks. This arrangement allows the drive shaft to be selected for maximum flexibility relative to the expected torque so that the spindle and ring can act as a self-centering bearing.

The inherent viscous heating problem is minimized by the thin film as well as by control of the temperature in both cylinders through the use of a common thermostatic fluid[7]. A sample calculation for this study by use of the modified equation[8],

$$\Delta T_{max} = \frac{n\dot{\gamma}^2 h^2}{8\ k_T} \tag{1}$$

shows an increase of only a fraction of a degree in the worst case, where $h = 1.1 \times 10^{-3}$ cm, $\dot{\gamma} = 5 \times 10^5$ sec^{-1}, $\eta = 1$ poise, and $k_T = 1.6 \times 10^4$ g-cm/sec^3 $^\circ$K for polystyrene in decalin solutions. The thermal conductivity of polyisobutene is not available in the literature. However, one would expect that it is of the same order of magnitude as polystyrene. All tests are carried out at ambient temperature (25°C.). The observed temperature rise is 0.6°C. in the concentrated system under prolonged shearing. Thus, the viscous dissipation can be considered unimportant .

Two spindles of gap clearance of 1.126×10^{-3} cm, spindle #1A, and 3.318×10^{-4} cm, spindle #3, are used. The corresponding equation for this geometry for shear rate is given as[8]

$$\dot{\gamma} = 0.1229 \frac{N}{h} \qquad (2)$$

where N is the rotational speed of the spindle in r.p.m.; h is the gap clearance in cm; 0.1229 is the instrument constant; and $\dot{\gamma}$, the shear rate, has the unit of sec^{-1}. The shear stress measured at outer cylinder is given as

$$\sigma = 631.2 \ \tau_v k \qquad (3)$$

where τ_v is the torque measured at 10" position on the torque arm in volts which is a result of amplification of transducer response; k is the transducer constant in g/volts; and again 631.2 is the instrument constant; σ, the shear stress, expressed in dimensions of dyne/cm^2.

The apparent viscosity, n, of the test film is simply the ratio of shear stress to shear rate.

$$\eta = \frac{\sigma}{\dot{\gamma}}$$ (4)

Gap calibration of spindle #1A and 3 is achieved by running standard oils over the rotational speed range. Gap width can be calculated by combining eq. (2), (3) and (4) if viscosity, torque, and speed are known. An average value is then taken and standard deviations are 5.5% and 3.8% observed for spindle #1A and #3, respectively. Using these average h values to calculate shear rates as eq. (2), a replot of log σ vs. log $\dot{\gamma}$ for the tested Newtonian fluids is shown in Figure I. Displacement of lines in the figure is due to the differing viscosities of the test fluids. Data of two spindles agree well in the shear rate range at two temperatures, 25° and 31°C.

II.C. Rheometrics Mechanical Spectrometer

The RMS-7200 Mechanical Spectrometer used is made by Rheometrics, Inc., N.J. A pair of coaxial rotational cone and stationary plate is used for measuring viscosity[10]. Shear rate is obtained by dividing rotational speed over cone angle as,

$$\dot{\gamma} = \frac{\omega}{\beta} \tag{5}$$

where $\dot{\gamma}$ is shear rate in sec^{-1}, ω is the rotational speed of the cone in rad/sec, and β is the cone angle in radian. Shear stress is converted from the measured torque at the plate as,

$$\sigma \quad 980.7 \; \tau \; \frac{3}{2\pi \; R^3} \tag{6}$$

where σ is the shear stress in dyn/cm^2, R is the platen radius in cm, and τ is the measured torque in g-cm. Apparent viscosity for the gap is again given by eq. (4) as ratio of shear stress over shear rate.

The assembly comprising the smallest cone, 0.01 rad (0.57^{o}), and a platen of 50 mm diameter is used for all samples except that some of the concentrated solutions are measured on 100 mm platen for improved sensitivity at low shear. The equivalent data at the two radii indicate a good reliability. The edge effects are considered unimportant due to the use of small gap angle[11]. Data are discarded when inertia and elastic effects, as material "squeeze-out", is observed.

II.D. Gel Permeation Chromatograph

A Waters Associates Model 200 Gel Permeation Chromatograph equipped with an automatic injection system is used for molecular weight determinations. The unit is equipped with columns of styragel beads of nominal pore size of 10^7, 3×10^5, 3×10^4, and 3×10^3 Å. The elution solvent is tetrahydrofuran and the flow rate is kept constant at 1.0 ml/min. Other conditions are temperature at 25°C. and sample concentration at 0.5 mg/ml or lower.

Polystyrene standards of narrow distribution (from Pressure Chemical Co. and Duke Scientific Co.) are employed for calibration. The universal calibration method of Grubisic, Rempp and Benoit[12] indicates that the separation process is based on hydrodynamic volume, $\tilde{[\eta]}M$, for polymer coils flowing through the column.

At constant temperature and solvent, the relationship as $[\eta]_a M_a = [\eta]_b M_b$ is hold for linear amorphous polymers a and b. Mark-Houwink Equations for polystyrene and polyisobutene in tetrahydrofuran at 25°C. are[13,14]

$$[\eta]_{PS/THF} = 2.489 \times 10^{-4} M_w^{0.6597} \tag{7}$$

and

$$[\eta]_{PIB/THF} = 3.95 \times 10^{-4} M_w^{0.65} \tag{8}$$

Thus, a calibration curve of $\log M_w$ vs. $V_{e,p}$ (peak elution volume in ml) for polyisobutene is obtained from polystyrene standards.

It is realized that the calibration curve of polystyrene standards shows a distinct higher slope for molecular weight higher than 2 million. Thus, the calibration curve is approximated by two linear step functions.

$$\log M_W = -0.0555 \, Ve + 12.7, \quad 5 \times 10^3 < M_W \leq 2 \times 10^6 \tag{9}$$

$$\log M_W = -0.1223 \, Ve + 20.48, \quad 2 \times 10^6 < M_W < \text{exclusion limit} \tag{10}$$

It is understood that the separation processes in the column should be continuous towards the exclusion limit. Eqs. (9) and (10) are approximations of this curve.

The manipulation for weight and number average molecular weight and the ratio is employed according to the Waters' Manual[15] by using calibration curve of eqs. (9) and (10). In practice, a computer program is used to resolve the data.

II.E.   Experimental Procedures

II.E.1.   Flow Curve Development

Some typical flow curves are shown in Figure 2 and 3. Low and intermediate shear rate data are obtained from the Mechanical Spectrometer. High shear data are collected from the High Shear Viscometer. All runs are at 25°C. Data from Spectrometer and Viscometer agree well and fall on a smooth curve. See Figure 2 and 3.

The homogeneous solution is placed in the gap between cone and plate according to the Rheometrics Manual[10]. Measurements are then started at the lowest shear rate with measurable torque. Torque readings are taken when they reached the steady state. Since high molecular weight polymers are used, the possibility of shear degradation is considered throughout. Shearing is performed stepwise from lowest to high shear rates with a frequent recheck at low shear. An arbitrary lower limiting value of shear rate is chosen for each run, so that a reproducible viscosity is always obtained to ensure no degradation products from previous runs at higher shear. In this manner, a flow curve is constructed progressively back and forth towards the highest possible shear. Flow instability in the cone and plate geometry has limited runs at higher shear before degradation can occur.

Low viscosity materials are tested up to 10^3 sec^{-1} at smallest cone angle due to the instrument stress limit. However, high visco-elastic materials tend to build up its elasticity at lower shear. For

example, polyisobutene L-140 at 10% concentration can only be sheared as high as 2.5 sec^{-1}. Data from Mechanical Spectrometer are shown in filled symbols in Figure 2 and 3. Not all data of polystyrene solutions are shown in order to avoid congestion. Some typical flow curves of these solutions represent the curve shape as well as the viscosity and shear rate range for the combination use of the Spectrometer and the Viscometer.

High Shear Viscometer is designed for shear rate above 10^3 sec^{-1} and for the features mentioned earlier. Flow curve development is then continued in this instrument provided that degradation is not observed. Operation of High Shear Viscometer is given in detail in Manrique's thesis[8]. Sample is pumped carefully into the gap, with spindle in place, through a syringe and the sample line. To make sure the gap is completely filled with sample, a pressure is applied to the syringe with a clamp. The spindle is then turned slowly by hand to help evenly distribute the test material into the gap by applied pressure. This procedure is continued until the sample appears on top of the ring gap. This is used as the first indication of a full gap. The clamp pressure is then removed. The spindle is connected to the drive and the assembly is ready for measurement. The normal force, though very small in thin gap, tends to push the sample up and down in the gap. A continuous feed of sample from sample line by vacuum effect will further reduce the possibility of incompletely filled gap. The

reproducible high and constant torque readings are used as a second measure of a full gap.

Primary criterion of shear degradation is permanent viscosity loss measured at low shear rate. This phenomenon is observed for high molecular weight samples of both polystyrene and polyisobutene at higher shear. Whenever a permanent viscosity loss is detected, prolonged shearing is carried out at that high shear rate until the torque dropped to a steady state value. The temperature rise was noted along this path. In some cases, this procedure took 20-30 minutes to reach steady state. The rapid drop in torque at the early stage and the subsequent levelling-off is a result of mechanical degradation. Thermal and oxidative modes of degradation are neither expected nor observed.

II.E.2.   Shear Degradation Measurements

All viscosity data obtained from the Mechanical Spectrometer are reversible as no permanent viscosity loss is noted. However, shear degradation as a result of permanent viscosity loss is found in the High Shear Viscometer. When this occurs, the spindle is taken from the barrel after the steady state torque is reached. The spindle is air dried in a ventilating hood and washed thoroughly with tetrahydro-furan. After proper filtration, the THF solution is collected and ready for GPC injection. Additional and equivalent THF solutions are also prepared from (a) the sample taken before reaching the gap,

"line-end sample", (b) the sample in the syringe before going into the line, "syringe sample", and (c) the sample prepared in the bottle, "solution sample". Control samples taken directly from supplier's jars are also prepared. All concentrations for GPC analysis are kept at 0.5 mg/ml in THF except those of the "spindle sample" which is much lower. These are, of course, the important samples.

The GPC instrument is operated at least 24 hours prior to testing to assure a constant temperature and flow rate. Flow rate is checked frequently and found to be 1.00 ml/min ± 2%. Detector sensitivity was set at 16x for spindle samples and 4x for the rest. For the highest sensitivity, 1bx, runs, 36 hours of warm-up is required to achieve a stable base line. The instrument is protected from any small external vibration, e.g. heavy foot-steps or slamming of the door. The molecular weight and its distribution thus measured are recorded in Tables III and IV.

C H A P T E R I I I

RESULTS AND DATA REDUCTION

III.A. Shear Degradation Results

III.A.1. General Comments

Both polystyrene and polyisobutene are found to degrade under high shear in laminar flow. No degradation is observed in data from the Mechanical Spectrometer because of the lower level of shear rates and stresses. In the High Shear Viscometer, care has been taken to evaluate and exclude degradation caused by pumping the polymer solutions into the gap between the cylinders. Essentially, the pumping is a capillary extrusion through the inlet tubing. The shear stress at wall can be made low by slow injection rates. However, there are several junctions along the injection line which connect tubes of different diameters. These junctions can cause entrance effects which may also lead to shear degradation[16]. Two extra samples are thus collected for each run. They are the syringe sample and the line-end sample. Results on these samples are included in Tables 3 and 4. As judged by both experimental values obtained, and direct comparison of chromatograms, shear degradation does not occur during injection pumping of sample into High Shear Viscometer.

Among the undegraded polymers, the average M_w and M_w/M_n obtained from GPC are listed in column 6 of Tables 3 and 4 for both polymers.

Standard deviation is shown as ± percentage after the mean value for polystyrene A and B and polyisobutene L-140 and L-100. Single data is used for polystyrene C and D and polyisobutene LM-MH. A good consistency is shown by the standard deviation from the GPC measurement and calculation.

The manufacturer's specification of polystyrenes are

$$\text{Polystyrene A:} \quad M_w = 7.1 \times 10^6, \quad M_w/M_n = 1.1$$

$$\text{Polystyrene B:} \quad M_w = 2 \times 10^6, \quad M_w/M_n = 1.2$$

$$\text{Polystyrene C:} \quad M_w = 6.7 \times 10^5, \quad M_w/M_n = 1.15$$

$$\text{Polystyrene D:} \quad M_w = 2.3 \times 10^5, \quad M_w/M_n = 1.06.$$

Polyisobutene polymers are expected to be near the most probable distribution due to the polymerization process.

When comparing experimental M_w to the manufacturer's specification, polystyrenes A, B, and D are 3, 15, and 6% higher, respectively; while polystyrene C is 17% lower. The experimental M_w/M_n values are almost as much as twice higher for polystyrenes A and B than the suppliers' data; while polystyrenes C and D are 36 and 15% higher. These variations are attributed to the assumption that column resolution is approximated by step linear functions towards the high molecular weights. The M_w values for polystyrenes B, C, and D are correlated well on the lower linear GPC calibration curve, i.e. eq. (9) in Chapter II. A more precise and complicated GPC manipulation method which takes into account the sigmoidal calibration curve and peak broadening correction will improve the results.

Slagowski[24] reported polystyrene of molecular weights higher than about 10^7 g/mole would be degraded under normal GPC elution conditions. In this work, polystyrenes A and B have high molecular weight tails in the order of 10^7, estimated by the corresponding eluent volume in the chromatogram by using the higher linear calibration curve, eq. (10) in Chapter II, to this region. A simplified calculation of highest shear stress at wall for connecting tubings between GPC columns is 480 dyn/cm^2. This is assumed below the critical stress for laminar shear degradation (cf. Figure 4). The possible turbulant flow in the pumping head, junctions of tubings, and the filter is suspected for the cause of degradation. If this is true then that will be the limit of use of GPC characterization. A high resolution GPC for high molecular weight polymers ranging from 10^6 to 10^7 using columns packed with small gel particles has been reported[25].

Although the difficulties of running high molecular weights in GPC has been explored, and remaining yet to be resolved, the main purpose of this study is to check the shear degradation accompanying high shear viscometry. That is, the changes in M_w and M_w/M_n are monitored carefully and further determine the regions of shear for which the materials are mechanically stable or unstable. By direct comparison of the M_w differences before and after shear, the sizable viscosity and M_w loss is attributable to shear degradation.

III.A.2 Polystyrene in Decalin Solutions

Shear degradation has been observed under high shear conditions in the High Shear Viscometer for polystyrene A, B, and C at high concentrations. (Table 3) Polystyrene D is mechanically stable over the full stress range. A double logarithmic plot of final value of M_w for the degraded polymer vs. shear stress at steady state is given for several concentrations in Figure 4. The molecular weights correspond to the maximum steady state degradation at each shear stress. The final molecular weights of sample D measured at different stresses lie below the straight lines distinguishing the mechanically stable and unstable region. The data suggest that one may develop a curve delineating the boundary of mechanical stability which can become a useful empirical correlation in applications involving shear fields.

III.A.3 Polyisobutene in Decalin Solutions

In a fashion similar to that for polystyrene solutions in decalin, degradation of this system is found only in the High Shear Viscometer and only for the two highest molecular weight samples, L-140 and L-100. Sample LM-MH is found to be stable over the full measurable shear stress range. See Table 4. Data points are insufficient to do a thorough analysis as in Figure 4. Porter and Johnson[19] have shown similar plots for polyisobutene in cetane. They use polymers of $M_v = 1.4 \times 10^6$ and 8×10^5, concentrations of 4~10%, and the same type of viscometer.

Their final molecular weights are determined internally by viscosity-molecular weight relationship.

10% Solutions of L-140 and L-100 are too viscous to pump through syringe and sample line in the Viscometer. Only 5 and 2% solutions are tested and then are found degraded. Flow curve development for these two concentrations are terminated so that the reported viscosities are reversible.

III.B.   Flow Curve Superposition

III.B.1   General Comments

Several parameters have to be evaluated before data superposition can be attempted. Zero shear viscosity, η_0, and the experimental relaxation time, τ_0, are the most important two. For η_0 the values are obtained experimentally except in some cases by extrapolation with the aid of Graessley's master curve[20] for the proper M_w/M_n. The data are listed in Tables 5 and 6. For τ_0 there are three conventional ways of estimation. One can choose τ_0 as the reciprocal of the shear rate at which η has dropped to some fixed fraction of η_0. Such a method is employed here and the fraction is chosen arbitrarily at 0.8. Alternative methods may take τ_0 as the reciprocal of the shear rate at intersection of extrapolation of two linear Newtonian and power-law portions or may assign τ_0 by superposition of the experimental data on a theoretical master curve of η/η_0 vs. $\dot{\gamma}\tau_0$. These methods require

a power law region to afford a meaningful interpretation. Our experimental flow curves, Figure 2 and 3, comprise a family of sigmoidal curves. Therefore, the first method takes the advantages of consistency.

III.B.2. Polystyrene in Decalin Solutions

Flow curves for each molecular weight are first normalized as log η/η_0 vs. log $\dot{\gamma}$. Using τ_0 as reciprocal value of $\dot{\gamma}$ at $\eta/\eta_0 = 0.8$, the curves are reduced again to log η/η_0 vs. log $\dot{\gamma}\tau_0/2$. The η_0 and τ_0 values are listed in Table 5. Reduced flow curves for solutions A, B, C and D are shown in Figure 5 to 8. The dotted curve represents the Graessley's master curve, with appropriate distribution, shifted to fit the experimental data. Superposition is good at low $\dot{\gamma}\tau_0/2$. However as $\dot{\gamma}\tau_0/2$ increases, deviation from Graessley's curve becomes more evident. The agreement of experimental data for 13% solutions of polystyrene A and B with entanglement theory is reasonably good over the measurable shear rate range. Slopes of the power law region for these two samples are identical to melt monodisperse polystyrene (0.82)[21].

Figure 11 is a plot of log η_0 vs. log C M_w. C M_w is used for convenience to evaluate the influence of the molecular entanglements[22,44]. The data points in Figure 11 are near the critical region for formation of entanglements. A slope of 4.5 is obtained for solutions of high

$C M_w$ values in Figure 11. The curve for solutions of low $C M_w$ values

can be approximated by a slope of 1.3 in the plot of $\log \eta_o$ vs. $\log C M_w$.

Figure 13 shows plot of $\log \tau_o$ vs. $\log C$. Straight lines can be

fit easily for samples B and C. Samples A and D do not afford linear

relationships. Further correlation of τ_R/τ_o to $C M_w$ is shown in Figure 14.

III.B.3. Polyisobutene in Decalin Solutions

The flow curves are reduced in the same manner as the polystyrene

solutions. Plots of $\log \eta/\eta_o$ vs. $\log \dot{\gamma} \tau_o/2$ for L-140 and L-100 are

shown in Figure 9 and 10. Data of η_o and τ_o are given in Table 6.

Dotted lines in each reduced plot represent Graessley's master curve

with individual M_w/M_n as measured in GPC. Good agreement at low reduced

shear rate is again achieved; nevertheless, a deviation from the master

curve is observed at low concentrations and at high shear rates. 5%

Solution of L-100 is the only case which approaches power-law behavior

giving a slope of 0.65.

Plots of $\log \eta_o$ vs. $\log C M_w$ and $\log \tau_o$ vs. $\log C$ are shown in

Figure 12 and 15, respectively. In Figure 15, data for solutions of

L-100 show good linear correlation in the concentration range, 2-10%,

in contrast to that for solutions of L-140.

Solutions of LM-MH are not shown because they lie below the crit-

ical entanglement region. The experimental relaxation time has no sig-

nificance in this case.

Plot of τ_R/τ_o vs. $C M_w$ for L-140 and L-100 is shown in Figure 16.

CHAPTER IV

DISCUSSION

IV.A. Shear Degradation

IV.A.1. General Comments

Homolytic rupture of main chain carbon bonds is generally found in mechanochemistry[4] and especially for the two polymers under study here. As macroradicals are the reactive species formed by stress, they can undergo chain transfer, recombination, and disproportionation depending on the reactivity of radicals and the environment. The probability of recombination is reduced because the macroradicals are separated beyond reaction distance by the same forces which produce rupture. By using radical acceptors in polystyrene, Baramboim[27] concluded no appreciable effect on the rate or extent of degradation. It is, thus, speculated that disproportionation is the major mode of radical termination which forms linear products. The other polymer, polyisobutene, is considered to be of high chemical purity, non-polar, and structurally linear, amorphous, and regular. It is also not prone to chemical crosslinking.

Mechanical mechanisms such as random or selective scissions have been proposed. Bueche[28] concluded the mid-chain rupture due to the highly concentrated stress in that chain region. An alternative random scission is commonly found in oxidative degradation. Scott[29] has

evaluated different criteria for random degradation of linear polymers.
He gives a correlation that predicts the relative decrease in weight
and number average molecular weight.

In this study, degradation is found for entangled systems. It is
believed that degradation occurs through the extending force on a net-
work of enmeshed polymer chains. Since the entanglement points can be
treated as randomly distributed in the system, breakage at the mid-
point between entanglements is expected to be random[4].

Temperature and solvent are constant factors in this study.
Decalin is reported as θ-solvent for polystyrene at 19.3°C. with trans
to cis ratio of 77 to 23[30]. Observations for polystyrene solutions
show an initiation of turbidity loss at a temperature of 18°C.; total
clarity occurs at 20°C. and above. The temperature of the experiment,
25°C., is near the θ-condition. A contracted coil conformation is
assumed. Turbidity is not observed for polyisobutene in decalin solu-
tions so low as 15°C. Investigation of the θ-condition for this pair
is not available in the literature.

IV.A.2 Molecular Weight and its Distribution

A decrease of molecular weight is a general feature of shear
degradation. In rare cases crosslinking and branching reactions can
predominate and lead to a molecular weight increase. The decrease in
molecular weight is usually rapid at first, then with the reaction

becoming slower until an apparent limiting molecular weight is reached.
The existence of the final molecular weights have been correlated with
shear stress under fixed conditions by Bueche[28].

In this study, polystyrene D shows a maximum of 3% variation in
terms of M_w's which are measured before and after severe shearing.
(See Table 3.) It is thus concluded that this molecular weight is mech-
anically stable over the experimental stress range. (See Figure 4.)
The other polystyrenes suffer progressively more degradation at higher
molecular weights. It is shown that the initial molecular weight does
not govern the final molecular weight.

For polyisobutene solutions, sizable loss of M_w is found for
L-140 and L-100. LM-MH has been concluded to have no degradation when
examining the molecular weight change. (See Table 4.) The final molec-
ular weight is also independent of initial molecular weight. Correla-
tion of this final molecular weight and the steady state shear stress
is reported for polyisobutene in cetane at 4~10%[19]. A linear relation-
ship is obtained at each concentration. In this study, only 2 and 5%
polyisobutene solutions are studied. To obtain a similar plot, one
needs more data.

When comparing M_w/M_n in Table 3 between values for undegraded and
degraded polymers, sample D can be concluded of not changing. Sample
C data does not change much perhaps since shear stress is near the
critical value as indicated in Figure 4. Samples A and B are difficult

to compare due to their high magnitudes and experimental errors. The changes of M_w/M_n in Table 4 are not appreciable since polyisobutene has an initially broad distribution. A non-selective degradation is possible for the above entangled systems. A definite conclusion would require further studies such as electron spin resonance.

IV.A.3 Concentration Effects

The influence of polymer concentration on the extent of shear degradation in solution is not sufficiently clear from available literature. In general, shear thinning and shear degradation can be considered as competitive processes which depend on temperature and the chain relaxation time. In an entangled system, chain breakage occurs perhaps near mid-way between two consecutive entanglement points before they can slip. Therefore, in concentrated solutions where entanglement is important, degradation of 2, 10, and 13% as shown in Figure 4 is positively dependent on concentration. The anomalies of 5% solutions may be due to experimental error. In general, the envelope defined by Figure 4 is fairly narrow over the concentration range. Normalization of concentration dependence is attempted by plotting stress axis as log σ/c, log σ/c^2, log σc and finally a plot of log M_w vs. log $\sigma/\sigma c$ indicates a good linear correlation; however, no immediate physical explanation can be drawn from this.

IV.A.4 Shear Stability Curve

Correlations between final molecular weight for shear degraded polymer and the steady state shear stress have been proposed in different forms by Bueche[28] and Harrington and Zimm[32]. Experimentally, semi-longarithmic plot of M_w and σ is used by Porter, Cantow and Johnson[33]; double logarithmic plot by Abdel-Alim and Hamielec[34]. Ram and Kadim[31] following the development of Harrington and Zimm, obtain a single parameter representing the minimum force required for degrading a polymer sample to its final state.

The shear stability curve in this study is plotted double logarithmically. The envelope of shear stability curves, in Figure 4, divides the mechanically stable and unstable region. High shear data for polystyrene D lie in the stable region so that both viscosity and molecular weight losses are not measurable. The intersection of initial molecular weight and shear stability curve is the critical stress locating the onset of shear degradation as a function of temperature, concentration, solvent and the particular shear mode in use. In this study, the shear stress recorded in the Mechanical Spectrometer is below the appropriate critical value and so within the stable region. It is also clear from the plot that initial molecular weight has effects only on the critical stress and rate of reaction. Final molecular weight is independent of its initial value in mechanical degradation.

IV.B.   Flow Behavior

Graessley's molecular entanglement theory[1] has been used to evaluate experimental flow curves for the solutions of polystyrene and of polyisobutene in decalin. As treated in Graessley's theory[20] the shape of flow curve is a function of molecular weight distribution, especially in the transition region from Newtonian to power-law portion. The theory does not treat the limiting high shear region. The master curves obtained are chosen with proper distribution of the polymers tested here. Good agreement in this transition region suggests the theory has been useful. However, the deviation from the theory beyond the transition makes power-law exponent predictions more inaccurate.

It is also noticed for solution viscosity that η_0 should be replaced by $\eta_0 - \eta_s$. Since the solvent viscosity of decalin is much lower than the zero shear viscosity of all solutions, except those of LM-MH. Use of η_0 instead of $\eta_0 - \eta_s$ is within experimental error. LM-MH solutions are not tested for superposition.

IV.B.1   Zero Shear Viscosity

Berry and Fox[35] have obtained a collective plot of log η_0 vs. log M_w for various linear polymers including polystyrene and polyiso-butene. They show straight lines of slope 1.0 and 3.4 with the intersection called critical molecular weight, M_c. The change of slope is continuous rather than an abrupt break over a decade of molecular weight.

The data and the graph are not affected by variations in the molecular weight distribution. When $M_w > M_c$, entanglements of polymer chains exist and determine the 3.4 power dependence. A review for polystyrene melt reported this power value from 3.1–4 according to different investigators[43]. When $M_w < M_c$, viscosity is a linear function of molecular weight in disentangled systems. The equivalent M_c for solution state is expected to vary inversely with the concentration. It is proposed that the product of $C\ M_w$ reflects the characteristic entanglement compositions in solution state[44]. Other workers[1,22] have also used $C\ M_w$ to correlate η_0. Polystyrene and polyisobutene solutions in this study are plotted in log η_0 vs. log $C\ M_w$ in Figure 11 and 12. In Figure 11, high $C\ M_w$ solutions are fitted with a least-square 4.5 slope. A distinct lower slope, 1.3, is drawn across for lower $C\ M_w$ solutions. It is clear that the concentrations and molecular weights chosen here are near the transition region. The extrapolated break point, 68,000, is compared to 50,500 for polystyrene solutions in n-butylbenzene at $30^\circ C.$[22]. The melt state data is 35,000[44]. In Figure 12 for polyisobutene solutions in decalin, slopes of 4.5 and 1.1 give the break point at 62,000. Porter and Johnson[36] reported 17,000 on absolute molecular weight scale for polyisobutene in cetane at $135^\circ C$. The high slope at high $C\ M_w$ axis is attributed to the concentration dependence of 4-5th. power at high molecular weights[23]. Ferry has suggested forms of $C\ M^{0.68}$ or $C^{1.47} M$ for η_0 function[23]. These cannot be confirmed for low molecular weight polymers used in this study.

IV.B.2 Experimental Relaxation Time

Relaxation processes are a characteristic of chain molecules. They depend on chain length, chain geometry, medium, temperature, and stress field. The longest relaxation time is usually employed to represent the processes rather than the full spectrum. Rouse derives the relaxation time, τ_R, based on bead-spring model with free draining condition. Graessley evaluates in his theory the maximum Rouse relaxation time with dependence on molecular weight at sufficiently low shear rates. It is presumed that each chain possesses a discrete set of relaxation times like that of an isolated Rouse chain. All are fixed fractions of the largest relaxation time.

At sufficient low macroscopic shear on an entangled system, random thermal motion as characterized by Rouse relaxation time can establish new couplings with incoming chain molecules as previous molecules leave. Thus, the topological state of the system remains the same as that at rest. This is the equilibrium situation envisioned in the Newtonian flow region.

For higher macroscopic shear rates, the time that potential couplings remain within the pervaded volume of a molecule will decrease. The time to form an entanglement as governed by the longest relaxation time is now shorter than the time of passing each potential coupling molecule as that governed by external shear rate. Accordingly the steady-state entanglement density of the system is expected to be a decreasing function of the shear rate.

In this study, the time constant at 80% drop from Newtonian behavior is selected to characterize the relaxation behavior. Its magnitude controls the time for formation of molecular chain entanglements between any molecules in the system and other molecules passing through its sphere of influence. Since the experimental relaxation time is near the Newtonian region, its value is of the order of the Rouse relaxation time, and hence it is determined both by the size of the chain and by the parameters of the medium.

Plots of log τ_0 vs. log C at constant molecular weight for polystyrene and polyisobutene solutions are shown in Figure 13 and 15, respectively. Polystyrene B and C are fitted with a linear relationship over the test range of 2-13%. Polystyrene A and D are less accurately fit to linear functions as indicated by the correlation coefficient. For polyisobutene, a good linear relationship is obtained for L-100 over the test range of 2~10%. Existed data of L-140 provides a less accurate linear correlation. LM-MH is not shown because the experimental relaxation time loses its meaning for disentangled solutions.

To check τ_0 against τ_R, plots of τ_R/τ_0 vs. C M_w are obtained for polystyrene and polyisobutene in Figure 14 and 16. In Figure 14 a tentative linear function is obtained across polystyrenes A and B. Figure 15 shows the best straight line for L-140 and L-100. Theoretically, one expects a linear relationship between τ_R/τ_0 for strongly entangled systems[46]. Experimental data with large error has been reported[45].

The scatter of data here is mainly because the test solutions are near the entanglement transition region. τ_R has inherent error originated from η_0. τ_0 has an experimental error inherent in its definition. Therefore, a combination of all errors shows up in both plots. Acquisition of more data points would be desirable to reduce the error.

IV.B.3 Reduced Flow Curves

Reduced flow curves for both polymers are shown in Figure 5~10 with Graessley's master curve drawn in dash line. The basis for Graessley's theory is the supposition that intermolecular chain entanglements control the magnitude of the viscosity and that the decrease in viscosity with increasing shear rate is caused by shear induced changes in the network of entanglements. Traditionally flow curves are developed on melts and concentrated solutions with shear rate seldom higher than 10^3 sec^{-1} due to the instrument stress limitation. In this study, most of the solutions are not strongly entangled as explained previously. The important contribution from high shear capability of high shear viscometer reveals clearly the flow curve approaches a limiting high shear value.

The lower the concentration or the higher the shear rate, the deviation from Graessley's entanglement master curve is more evident. Take polystyrene A as an example (Figure 5). Data for a 5% solution agree very well with the Graessley's master curve. The power-law

exponent is identical to that for monodisperse polystyrene melts[21].

Data for the 2% solution agree well only at reduced shear rates, $\dot{\gamma}\tau_0/2$, smaller than σ, while data for a 1% solution can only agree at reduced shear rates less than 2. This phenomenon is true for other molecular weights. Deviation from the entanglement curve begins earlier at lower concentrations as high shear limits are more readily approached. The changes in entanglement density at low concentrations due to the shear interaction cannot be significant because it is initially low. Flow curve of 1% solution of polystyrene A does level off at higher shear rates and the second Newtonian viscosity, η_∞, is approached. Yet η_∞ is difficult to obtain experimentally since shear degradation and secondary flow vortices will become important before η_∞ can be reached[38]. This deviatory phenomenon is also evident for polyisobutene solutions. (Figure 9 and 10.) Higher concentrations of L-140 and L-100 are not shown since these materials are too viscous to put into the thin gap.

Kirschke and Mewes[38] offer a trial-and-error method to find η_∞. Talbot[41] tries the asymptotic approach to predict η_∞ by using numerical analysis of a defined error function. These two methods are not attempted here owing to the lack of a profound theoretical justification.

Ito and Shishito[3,39,40] study the flow curves of polydimethylsiloxane melts and its solutions in petamer siloxane, as well as commercial and narrow distribution polystyrene in diethyl phthalate. The data are obtained from their specially designed capillary rheometer

which has shear range of $10^{-2} \sim 10^{6}$ sec^{-1}. Reversible viscosity is claimed for all measurements prior to the onset of melt fracture. They observed the deviation from Graessley's master curve in all cases. After introducing a shear-independent frictional viscosity, η frict. = $\eta - \eta_{ent.}$, into Graessley's theory, one can superpose the flow curves by plotting log $\eta_{ent.}/\eta_{ent.,o}$ vs. log $\dot{\gamma}\tau_{r}'/2$, where $\tau_{r}' = 6 (\eta_{o} - \eta_{frict})$ $M_{w}/\pi^{2} CRT$. This method is not attempted here since η_{frict} was obtained by trial and error method to fit Graessley's master curve. The frictional viscosity here cannot be clearly defined. Their choice of solvent of chemical structure comparable to the test polymer signifies the evaluation of friction. The friction action in this study is much more complex to afford valid treatment, because of the polymer and solvent interactions.

An alternative approach, perhaps allowing superposition, is to plot log $(\eta - \eta_{\infty})/(\eta_{o} - \eta_{\infty})$ vs. log $\dot{\gamma}\tau_{o}'/2$, where τ_{o}' is related to the form of $(\eta_{o} - \eta_{\infty})$ MW/CRT. This interpretation examines the fractional change of viscosity between its two Newtonian limits. The η_{∞} here can be estimated graphically from log η_{o} vs. log C M_{w} plot. A theoretical implication is that the lower Newtonian region, AE,

log CM$_W$
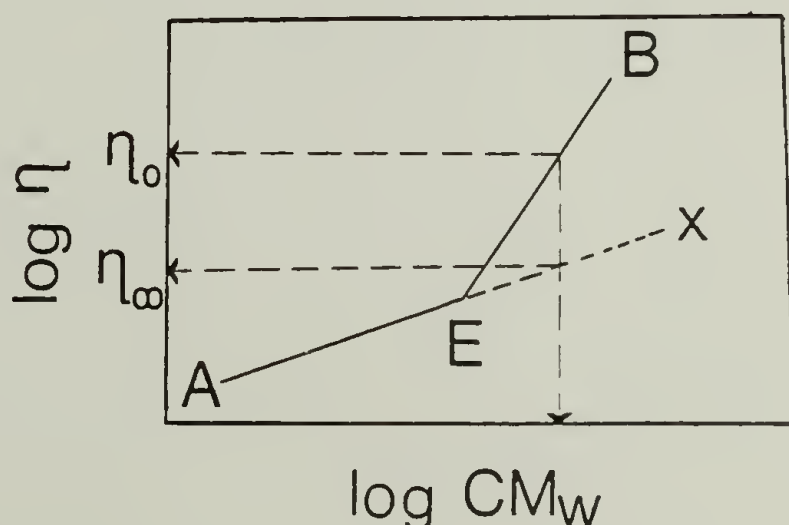
is continued and extended to the upper Newtonian region, EX, by compensation of shear action. The slope of upper Newtonian curve is expected to have the same slope of the lower Newtonian region.

Trials using this method for this study have not been successful since the data of both polymer solutions here are insufficiently definitive to extrapolate to high values of $C M_w$ axis; because the solution ranges are near the entanglement transition and so errors are large (Figure 11 and 12). Both higher and lower $C M_w$ solutions are desirable for this approach.

It has been shown that all the three LM-MH solutions lie below the critical entanglement region. The two polystyrene solutions of lowest $C M_w$ values, 2% of D and 5% of C, are expected to behave so as judged from Figure 11. However, weak non-Newtonian behavior has been observed for the five above solutions. Although the effect is small, this phenomenon may be a consequence of viscous heating seen at high shear rates. Other workers[40] treated this problem as a result of excluded volume effect.

Williams[42] in his review article has discussed the contributions to viscosity besides entanglement effect. They are the hydrodynamic interaction, internal viscosity, spring coefficient, and solvent power. These relative contributions to the apparent viscosity become definitely important at higher shear rates, especially in the upper Newtonian region. Greater understanding of these subjects in molecular rheology is necessary to interpret the experimental deviation from the entanglement theory.

CHAPTER V

APPENDIX

V.1 Notation

Symbol	Explanation	Unit
c	concentration	g/ml
σ	shear stress	dyn/cm^2
σ	steady state shear stress	dyn/cm^2
$\dot{\gamma}$	shear rate	sec^{-1}
η	apparent viscosity	poise
η_0	zero shear viscosity	" "
η_s	solvent viscosity	" "
η_∞	high shear limiting viscosity	" "
$[\eta]$	intrinsic viscosity	dl/g
HSV	High Shear Viscometer	—
RMS	Rheometrics Mechanical Spectrometer	—
GPC	Gel Permeation Chromatograph(y)	—
τ	torque	g-cm
τ_v	torque measured in volt as in HSV	volt
τ_0	experimental relaxation time	sec.
τ_R	Rouse relaxation time $6(\eta_0 - \eta_s)M_w/\pi^2 CRT$	sec.
h	gap width between cylinders in HSV	cm
N	spindle rotational speed in HSV	rpm
ω	cone rotational speed in RMS	rad/sec.
β	cone angle	rad.
T	temperature	$^\circ K$
k_T	thermal conductivity	$g\text{-}cm/sec^3 \; ^\circ K$

Symbol	Explanation	Unit
k	transducer constant in HSV	g/volt
R	platen radius	cm
V_e	GPC elution volume	ml
M_w	weight average molecular weight	g/mole
M_w/M_n	molecular weight distribution	—
M_c	critical molecular weight for entanglements	g/mole
$M_{w,i}$	initial molecular weight	g/mole
$M_{w,f}$	final molecular weight of the polymer which is shear degraded to a steady state	g/mole

V.2 Tables

TABLE 1

Test Polymers and Solvents

Polymer	$\underline{M_w}^*$	$\underline{M_w/M_n}^*$	Manufacturer
Polystyrene A	7.32×10^6	2.39	Duke Scientific Co.
" " B	2.27×10^6	2.63	Pressure Chemical Co.
" " C	5.56×10^5	1.57	" "
" " D	2.44×10^5	1.22	" "
Polyisobutene L-140	3.29×10^6	3.93	Exxon (Enjay) Chemical Co.
" " L-100	2.65×10^6	4.17	" "
" " LM-MH	7.83×10^4	4.32	" "

*values obtained from calibrated GPC analysis

Solvent	Specification	Manufacturer
Decalin (Purified)	cis/trans = 45:55	Fisher Scientific Co.
Tetrahydrofuran (Certified)	b.p. = $65.8^-66.0^{\circ}$C.	" "

TABLE 2

High Shear Viscometer Calibration Fluid

Fluid	Specification	Manufacturer
Ethylene Glycol	Reagent Grade, 19 cp. at 25°C.	Eastman Kodak Co.[1]
Cannon #S-20	30.32 cp. at 25.0°C.	Cannon Instrument Co.[2]
Fluid 100	98.0 cp. at 25°C.	Brookfield Engineering Lab. [3]

(1) Rochester, New York

(2) State College, PA

(3) Stoughton, MA

TABLE 3

Molecular Weight and Molecular Weight Distribution of
Polystyrene, a Function of High Shear History in Decalin

Sample	c,g/ml	Solution	Syringe	Line-end	Undegraded (avg.)	Spindle	Stress at Steady State, dyn/cm^2
A 7.32×10^6 2.39	0.0504	7.25×10^6 2.37	7.41×10^6 2.47	7.34×10^6 2.39	7.34×10^6 $\pm 1.7\%$	1.24×10^6 2.74	1.0×10^4
	0.0201	7.59×10^6 2.25	7.23×10^6 2.31	7.30×10^6 2.34	2.36 $\pm 3.0\%$	1.06×10^6 2.30	3.02×10^4
B 2.27×10^6 2.63	0.102	2.31×10^6 2.37	2.28×10^6 2.31	2.26×10^6 2.39	2.31×10^6 $\pm 1.8\%$	8.66×10^5 2.34	2.7×10^4
	0.0501	2.35×10^6 2.61	2.34×10^6 2.43	2.35×10^6 2.57	2.48 $\pm 5.2\%$	6.24×10^5 2.72	2.59×10^4
C 5.56×10^5 1.57	0.132	—	—	—	—	4.33×10^5 1.71	4.80×10^4
	0.102	—	—	—	—	5.22×10^5 1.69	4.43×10^4
D 2.44×10^5 1.22	0.133	—	—	—	—	2.43×10^5 1.25	6.81×10^4
	0.103	—	—	—	—	2.42×10^5 1.26	6.52×10^4
	0.0505	—	—	—	—	2.37×10^5 1.35	4.05×10^4

In the bracket, the upper value is M_w and the lower value is M_w/M_n; as both obtained from calibrated GPC analysis.

TABLE 4

Molecular Weight and Molecular Weight Distribution of Polyisobutene, a Function of High Shear History in Decalin

Sample	c,g/ml	Solution	Syringe	Line-end	Undegraded (avg.)	Spindle	Stress at Steady State, dyn/cm²
L-140 3.31×10^6 3.93	0.0508	3.19×10^6 3.78	3.35×10^6 4.03	3.31×10^6 3.97	3.29×10^6 $\pm 2.1\%$	2.15×10^6 3.74	2.10×10^4
	0.0203	—	—	—	3.93 $\pm 2.7\%$	1.79×10^6 3.79	2.65×10^4
L-100 2.70×10^6 4.01	0.0506	2.65×10^6 3.84	2.58×10^6 4.67	2.65×10^6 4.17	2.65×10^6 $\pm 1.9\%$	2.29×10^6 4.40 1.26×10^6 5.41	1.83×10^4 2.00×10^4
	0.0206	—	—	—	4.17 $\pm 8.5\%$	1.06×10^6 3.91	2.60×10^4
LM-MH 7.83×10^4 4.32	0.102	—	—	—		8.00×10^4 4.41	4.66×10^4

In the bracket, the upper value is M_w and the lower value is M_w/M_n; as both obtained from calibrated GPC analysis.

TABLE 5

Flow Parameters of Polystyrene in Decalin

M_w	c, g/ml	$C\ M_w$	n_0, poise	τ_0, sec.	τ_R/τ_0
A	.0504	3.69×10^5	1.00×10^3	4.0	8.91×10^{-1}
7.32×10^6	.0201	1.47×10^5	5.80	4.65	5.18×10^{-2}
	.0101	7.39×10^4	1.00	1.15×10^{-2}	—
B	.132	3.00×10^5	4.80×10^3	4.88	4.15×10^{-1}
2.27×10^6	.102	2.32×10^5	1.30×10^3	2.00	3.55×10^{-1}
	.0501	1.14×10^5	3.50×10^{-1}	2.08×10^{-1}	1.76×10^{-2}
	.0200	4.54×10^4	8.80×10^{-2}	9.09×10^{-3}	—
C	.132	7.33×10^4	3.35×10^1	7.25×10^{-3}	4.78×10^{-2}
5.56×10^5	.102	5.67×10^4	1.15×10^1	2.86×10^{-3}	5.38×10^{-2}
	.0504	2.80×10^4	1.10	5.05×10^{-4}	—
	.0202	1.12×10^4	2.30×10^{-1}	3.55×10^{-5}	—
D	.133	3.24×10^4	3.6	4.42×10^{-4}	—
2.44×10^5	.103	2.51×10^4	1.5	1.35×10^{-4}	—
	.0505	1.23×10^4	3.1×10^{-1}	5.85×10^{-5}	—

TABLE 6

Flow Parameters of Polyisobutene in Decalin

$\underline{M}_w$	c, g/ml	C $\underline{M}_w$	η_0, poise	τ_0, sec.	τ_R/τ_0
3.29×10^6 L-140	.102	3.39×10^5	8.00×10^3	1.47×10^1	4.31×10^{-1}
	.0508	1.68×10^5	4.20×10^2	3.13×10^{-1}	2.14×10^{-1}
	.0206	6.82×10^4	8.4	7.58×10^{-2}	4.34×10^{-1}
2.65×10^6 L-100	.102	2.84×10^5	3.80×10^3	3.69	6.68×10^{-1}
	.0506	1.40×10^5	1.45×10^2	4.29×10^{-1}	4.42×10^{-1}
	.0206	5.70×10^4	3.30	1.00×10^{-2}	1.05×10^{-1}
7.83×10^4 LM-MH	.102	8.01×10^3	9.80×10^{-1}	—	—
	.0503	3.94×10^3	2.00×10^{-1}	—	—
	.0203	1.59×10^3	8.00×10^{-2}	—	—

Figure 1. Shear Stress (log σ) versus Shear Rate (log γ̇) for Newtonian Fluids Measured on High Shear Viscometer
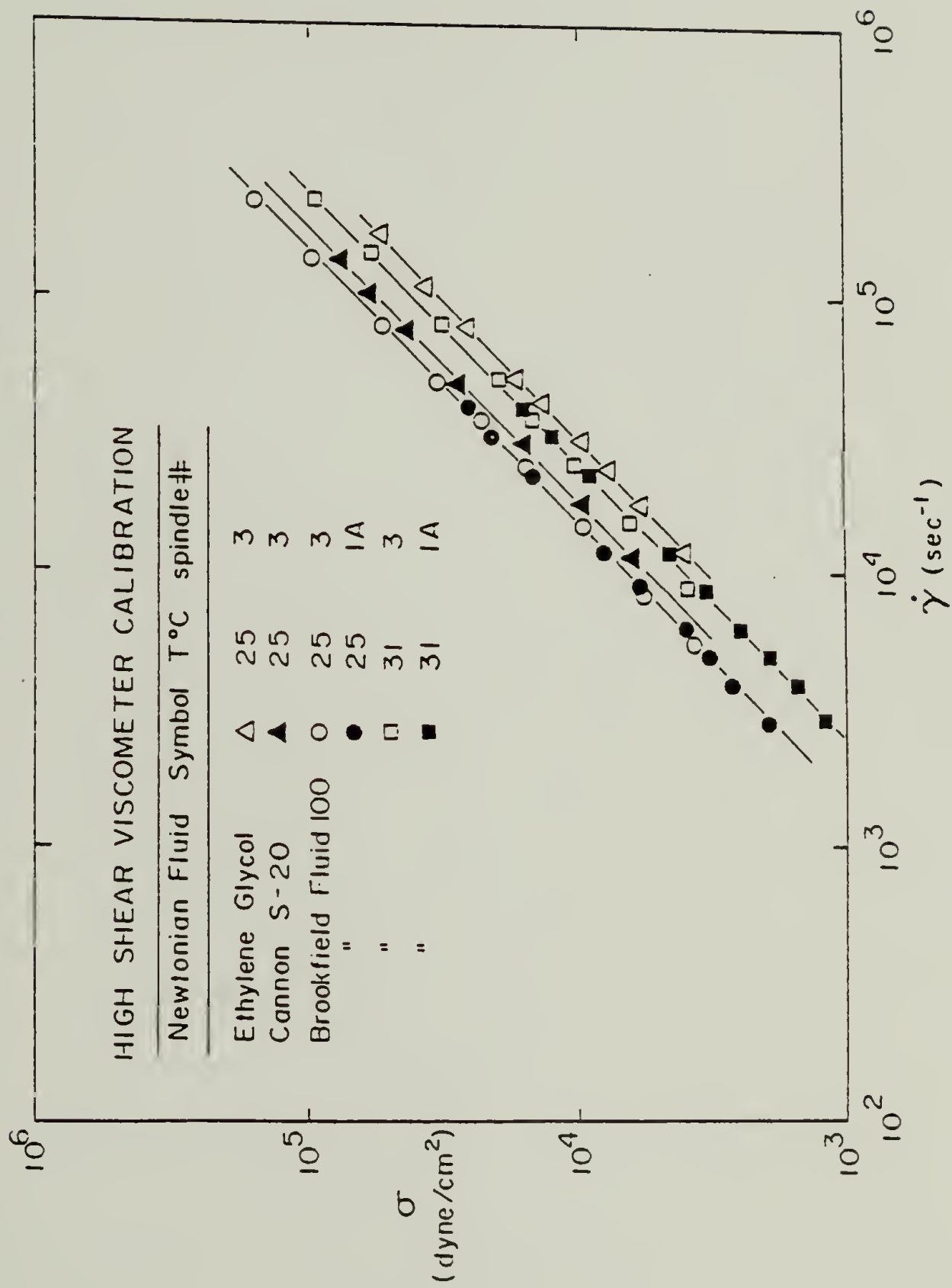
Figure 2. Viscosity (log η) versus Shear Rate (log γ̇) for Polystyrene Solutions
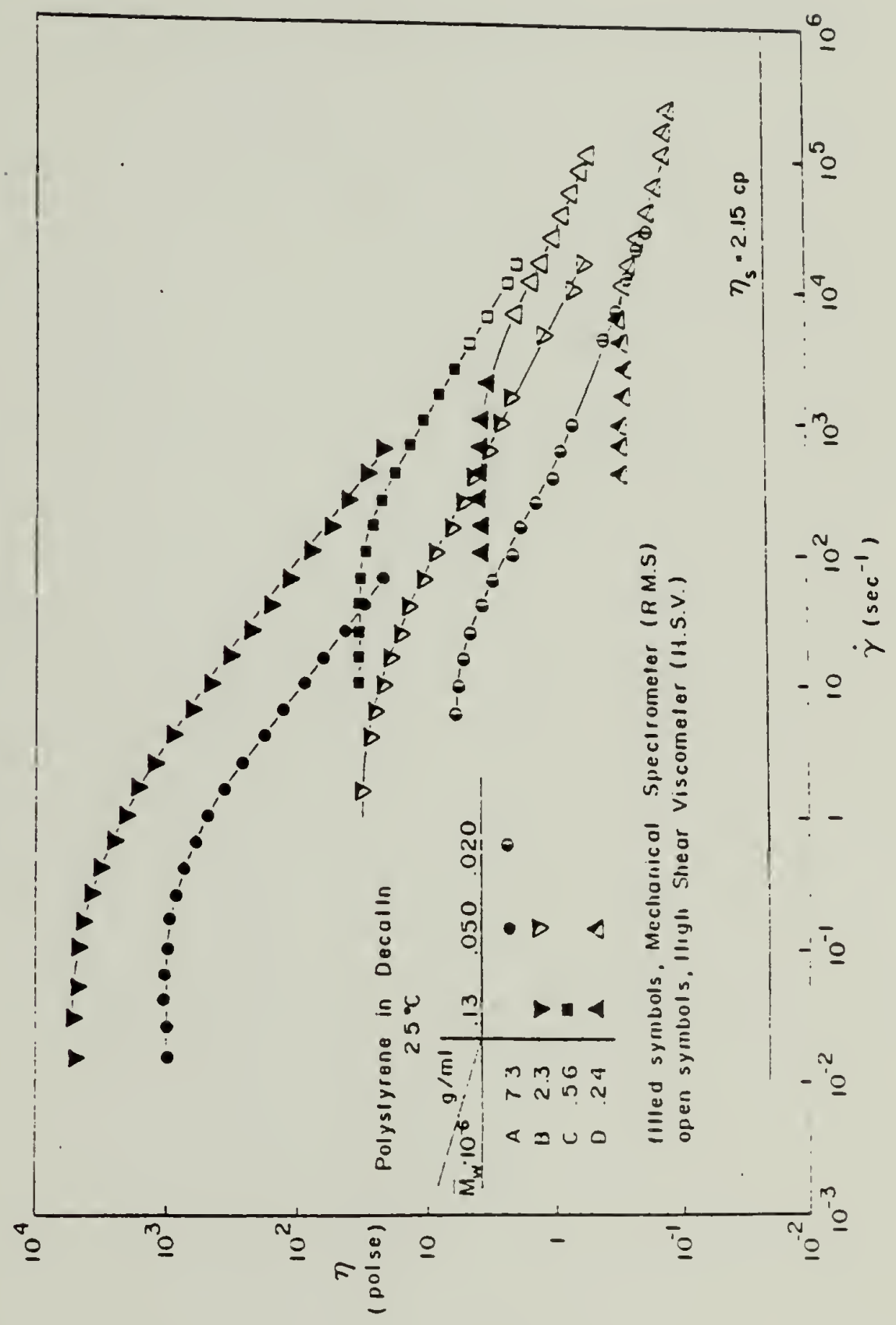
Figure 3. Viscosity (log η) versus Shear Rate (log γ̇)
for Polyisobutene Solutions
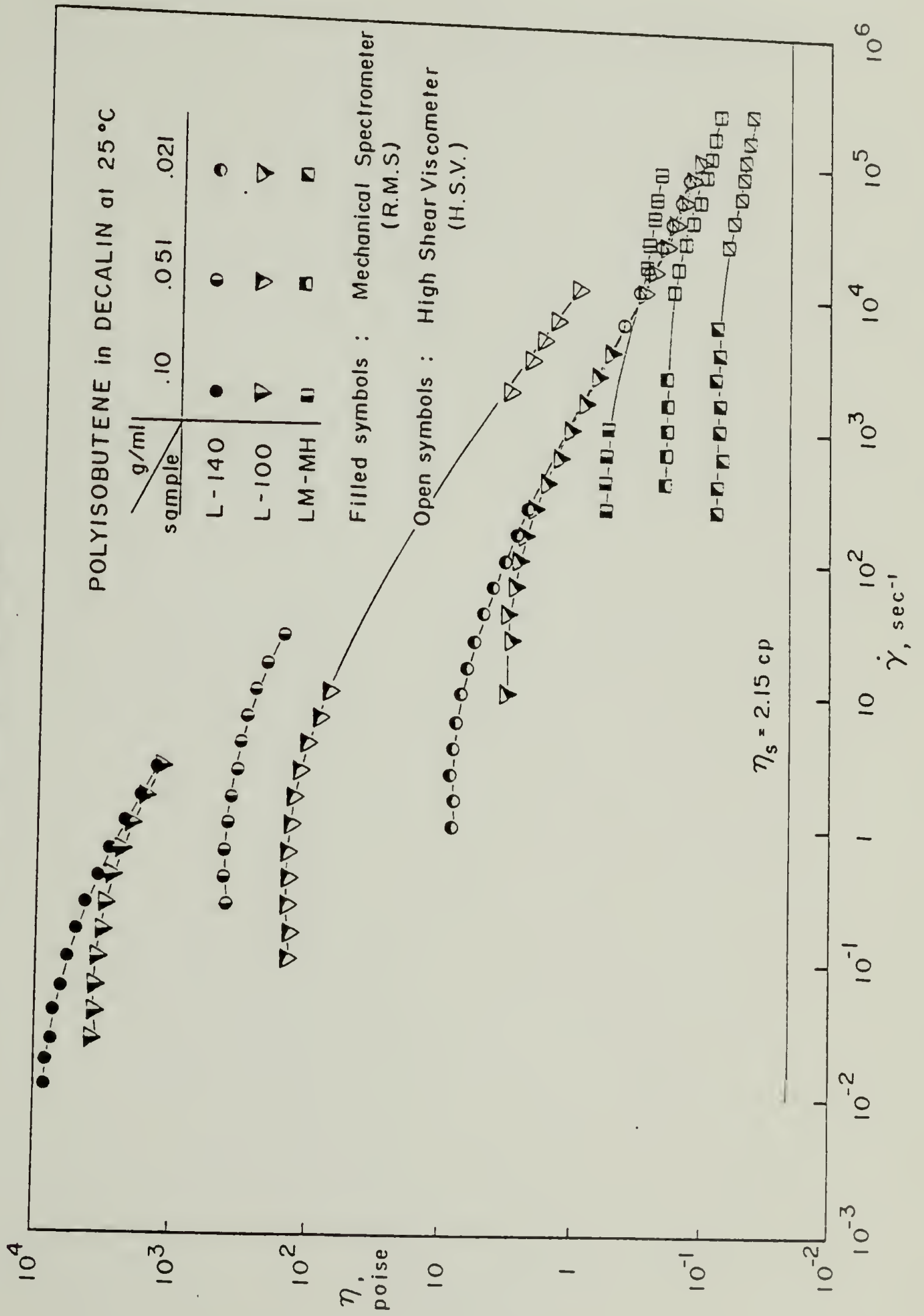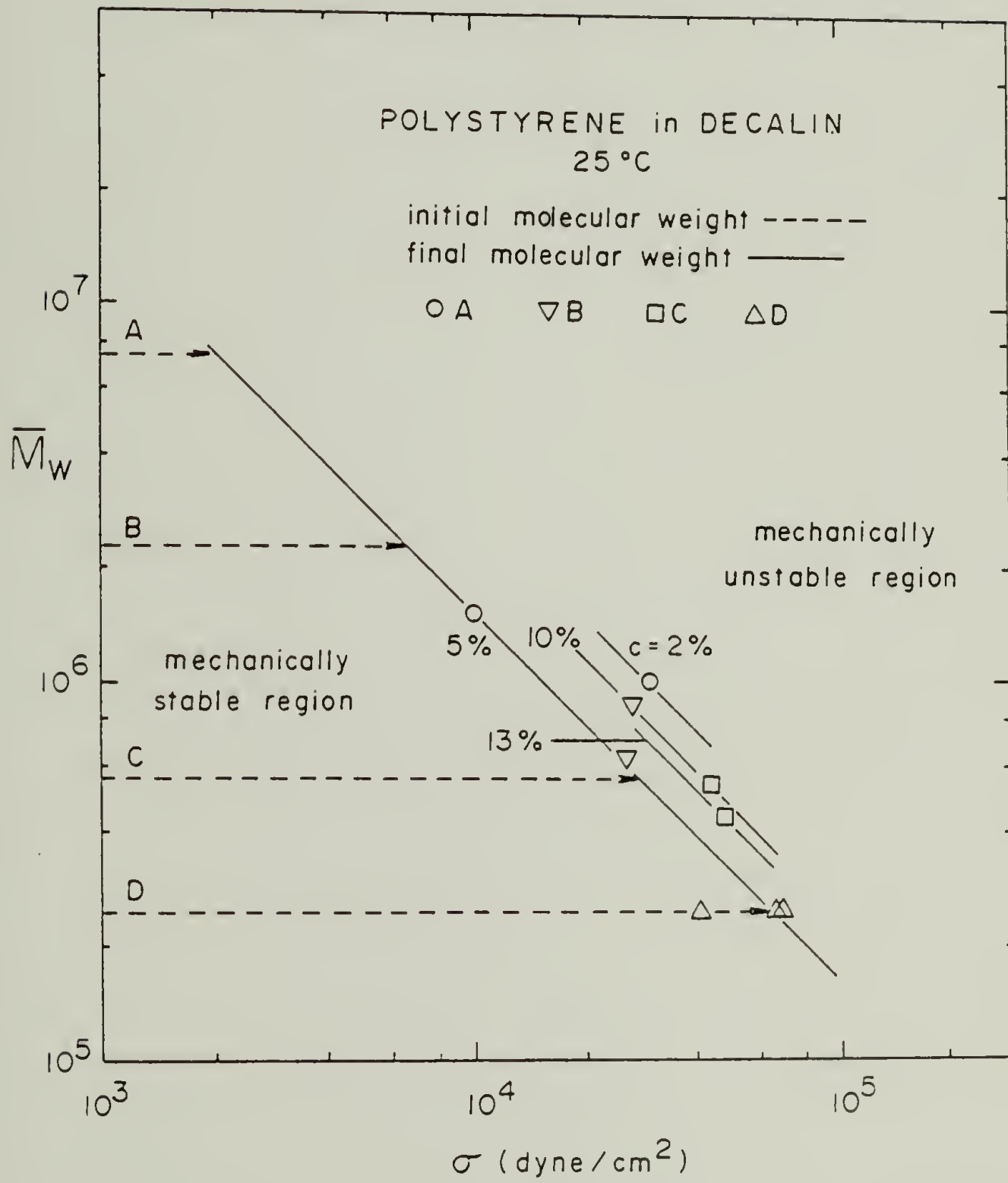
Figure 4. Shear Stability Curve for
Polystyrene Solutions
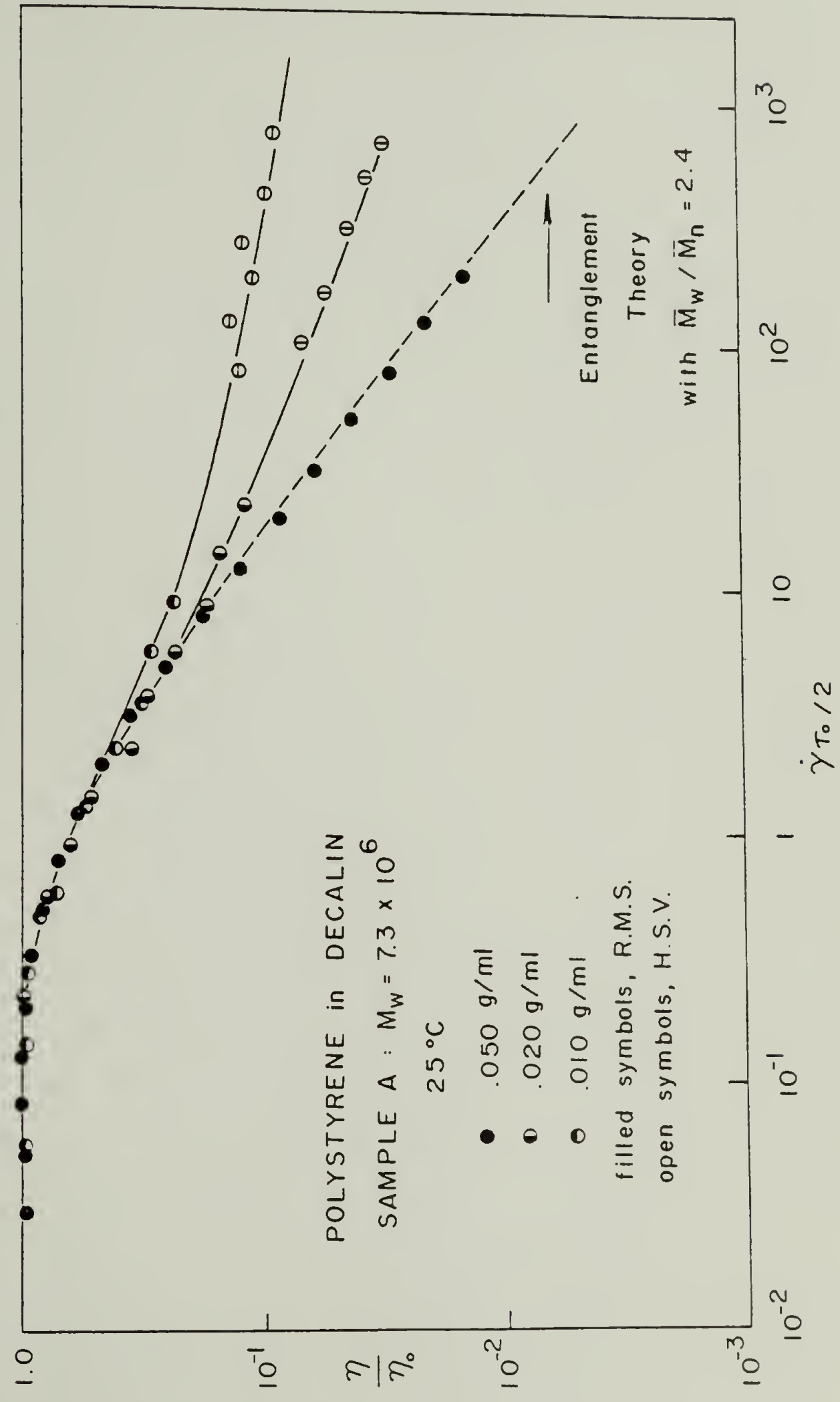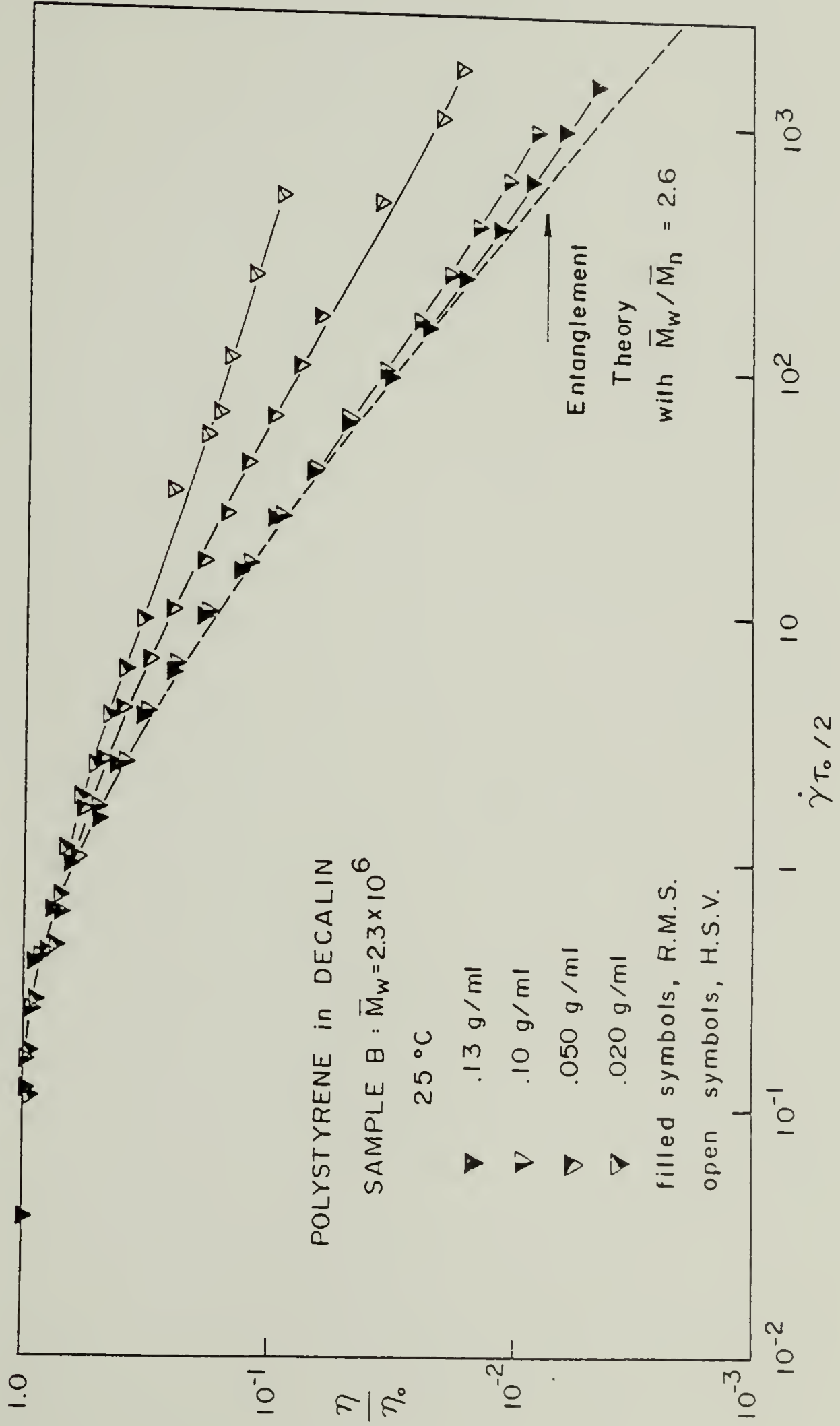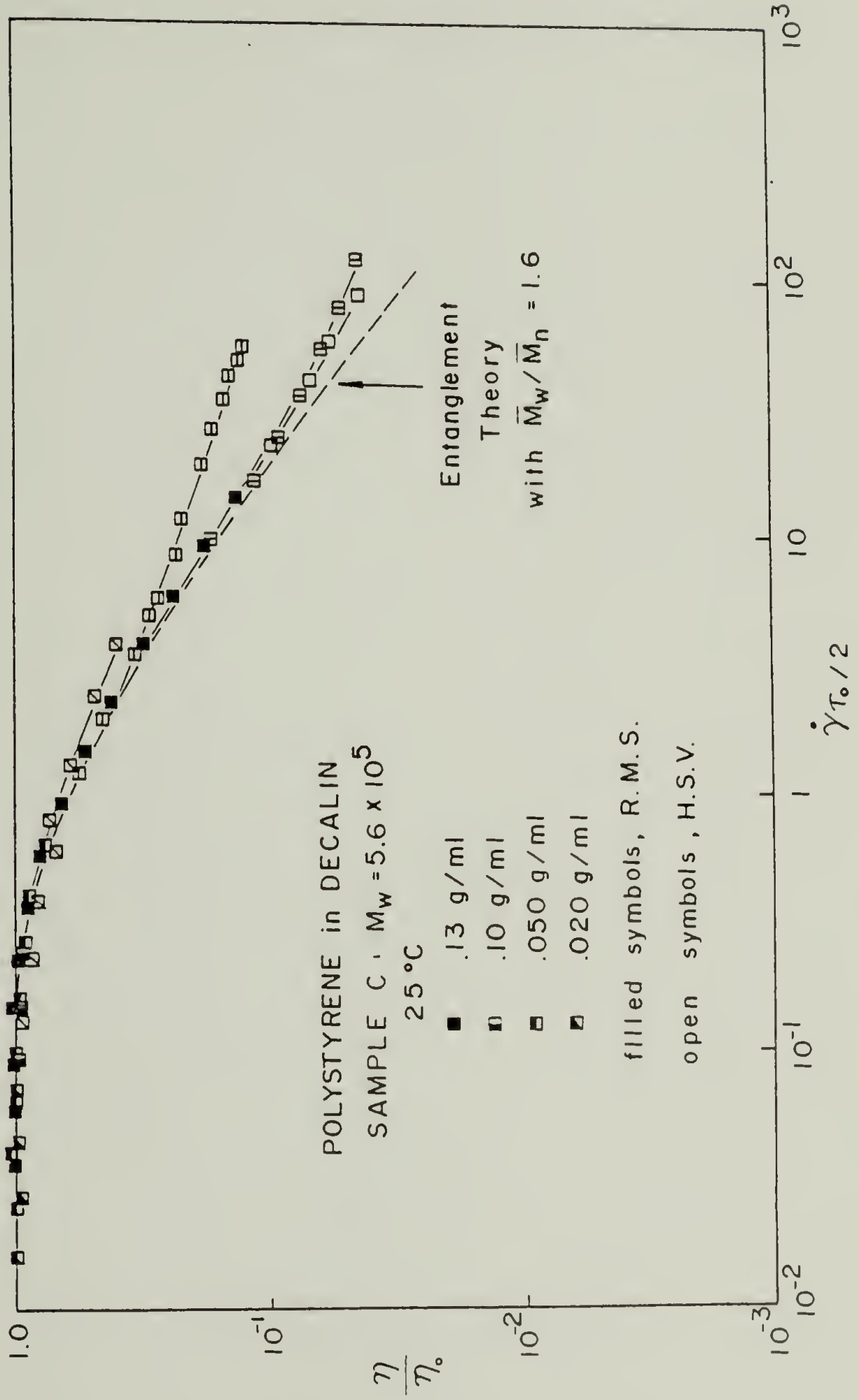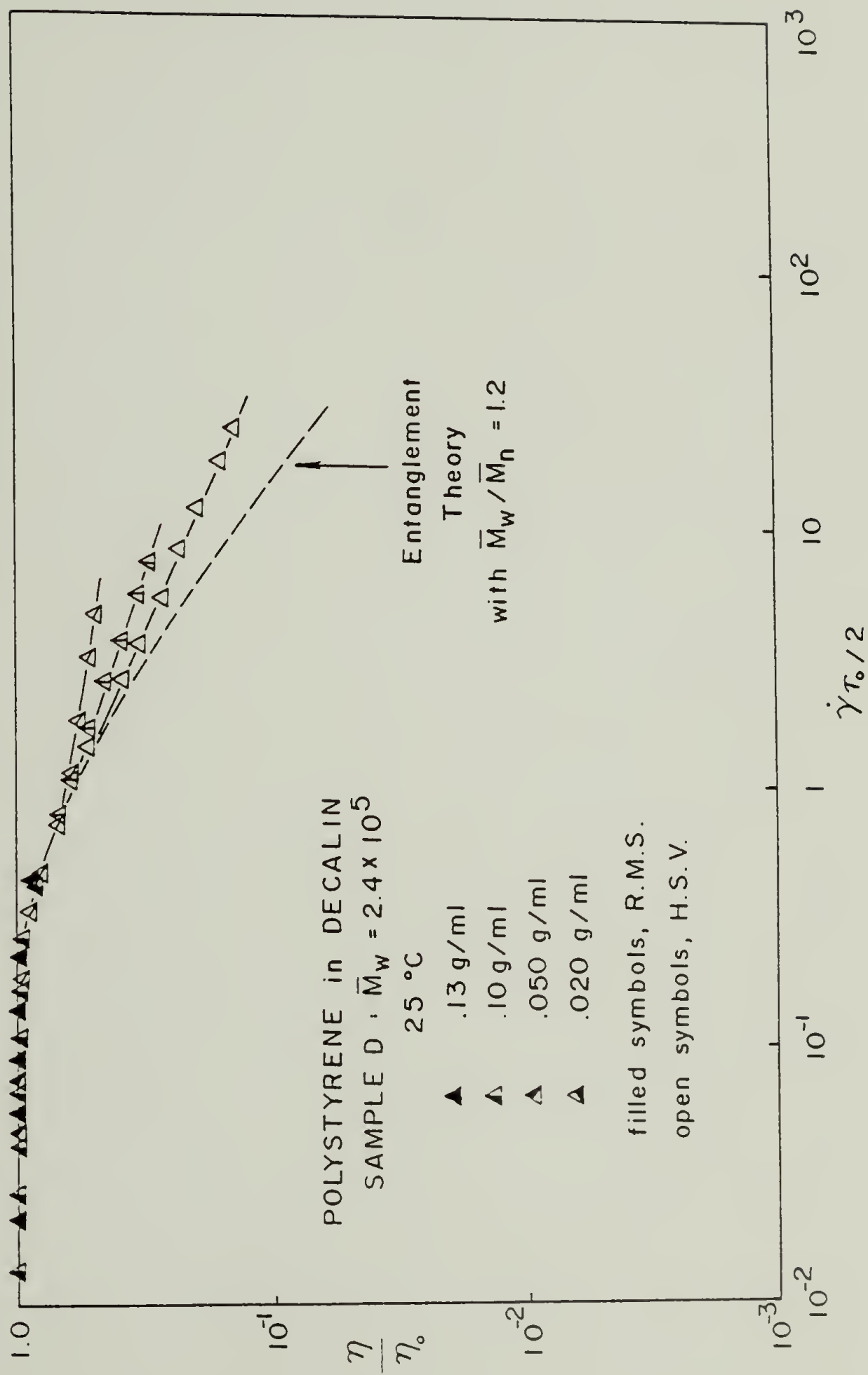
Figure 5. Reduced Flow Curves for Polystyrene A Solutions

POLYSTYRENE in DECALIN

SAMPLE A : $M_w = 7.3 \times 10^6$

25 °C

● .050 g/ml
◐ .020 g/ml
◒ .010 g/ml

filled symbols, R.M.S.
open symbols, H.S.V.

Entanglement Theory

with $\overline{M}_w / \overline{M}_n = 2.4$

$\dot{\gamma}\tau_o / 2$

$\dfrac{\eta}{\eta_o}$

Figure 6.   Reduced Flow Curves for Polystyrene B Solutions

Figure 7. Reduced Flow Curves for Polystyrene C Solutions

Figure 8. Reduced Flow Curves for Polystyrene D Solutions

Figure 9. Reduced Flow Curves for Polyisobutene L-140 Solutions
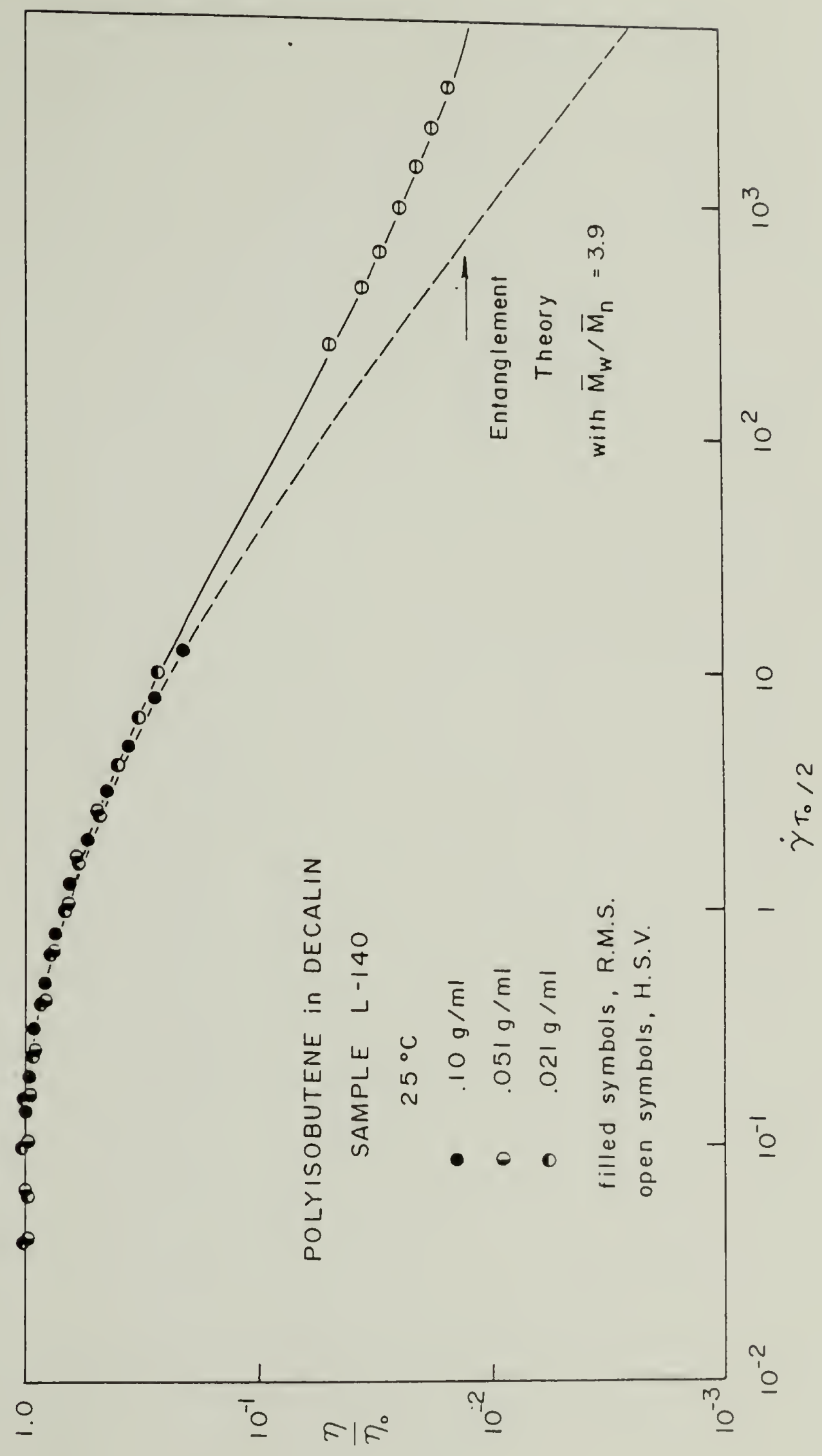
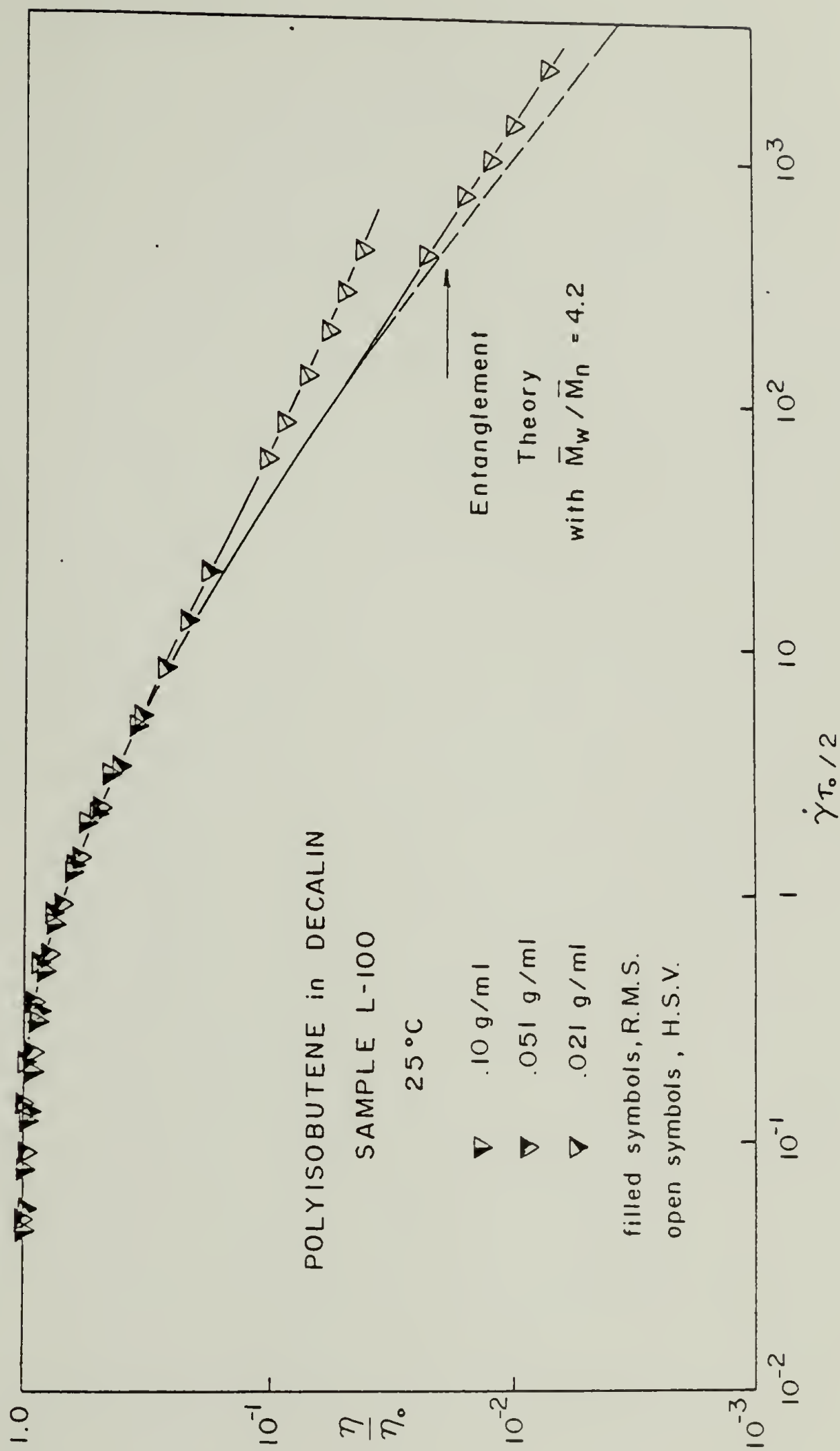Figure 10. Reduced Flow Curves for Polyisobutene L-100 Solutions

Figure 11. Zero Shear Viscosity ($\log \eta_0$) versus Product of Concentration and Molecular Weight (CM_w in g/ml·8/mole) for Polystyrene Solutions
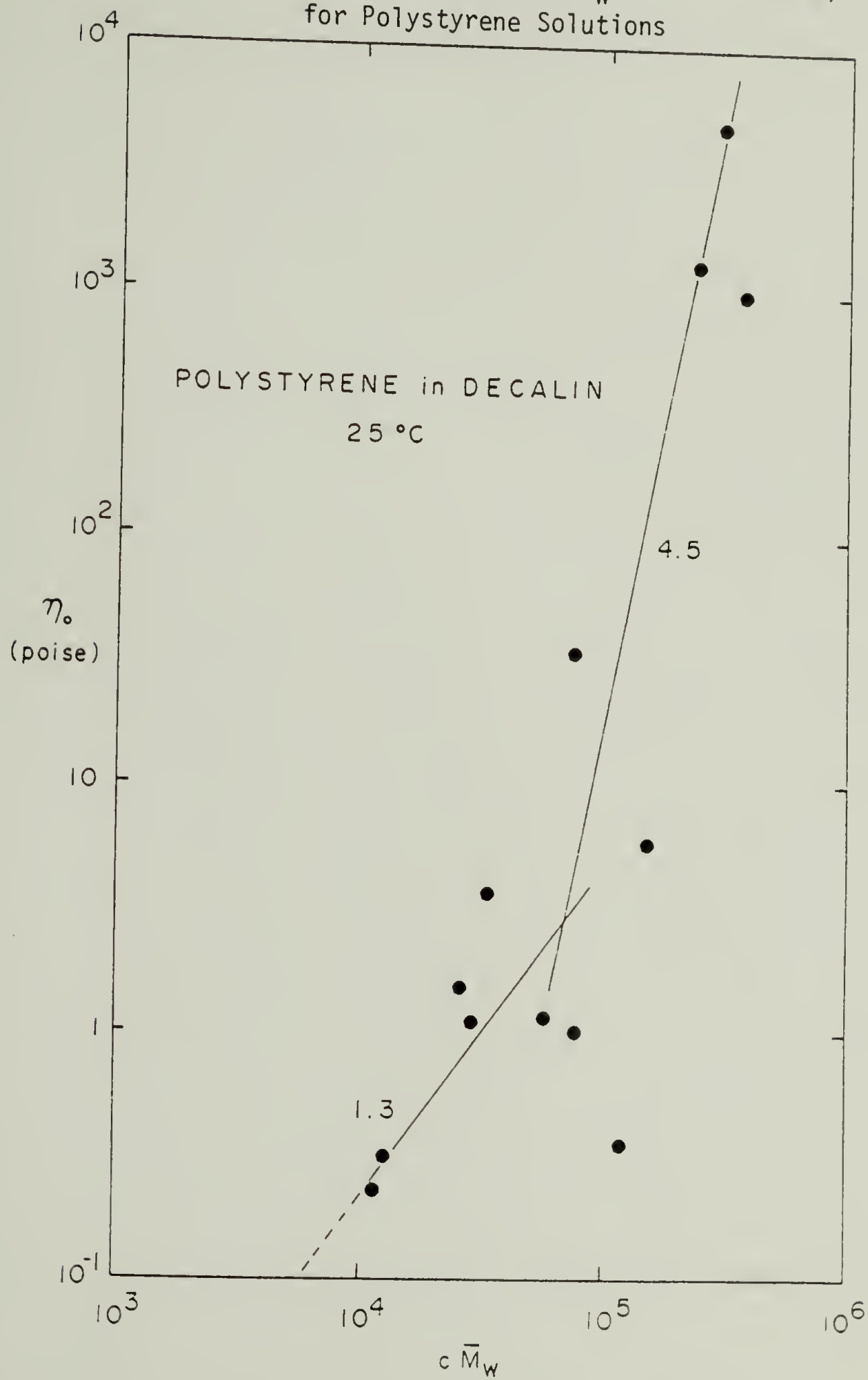
Figure 12. Zero Shear Viscosity (log n_0) versus
Product of Concentration and Molecular Weight
(CM_w in g/ml·g/mole) for Polyisobutene Solutions

Figure 12. Zero Shear Viscosity (log n_0) versus Product of Concentration and Molecular Weight (CM_w in g/ml·g/mole) for Polyisobutene Solutions
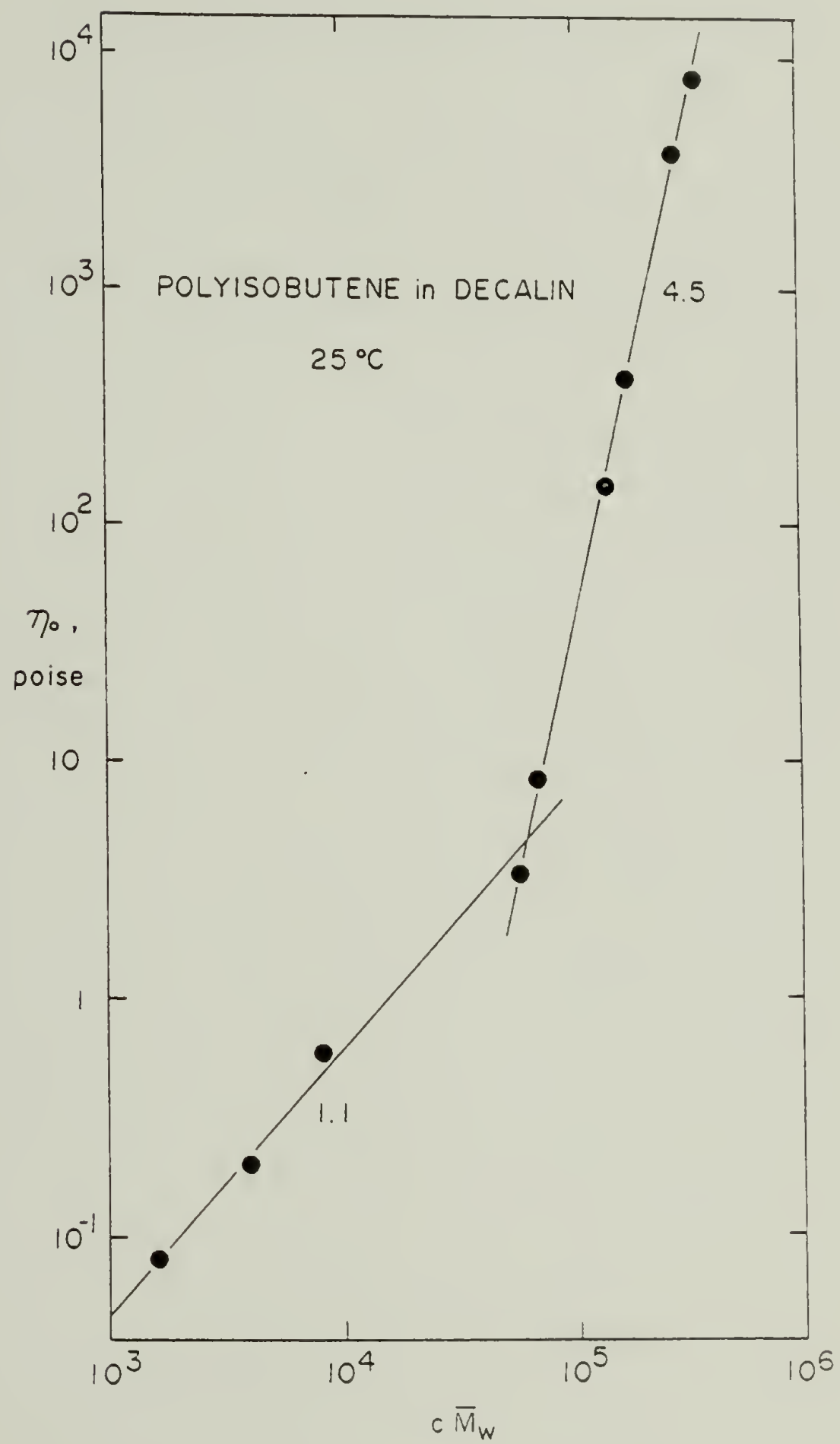
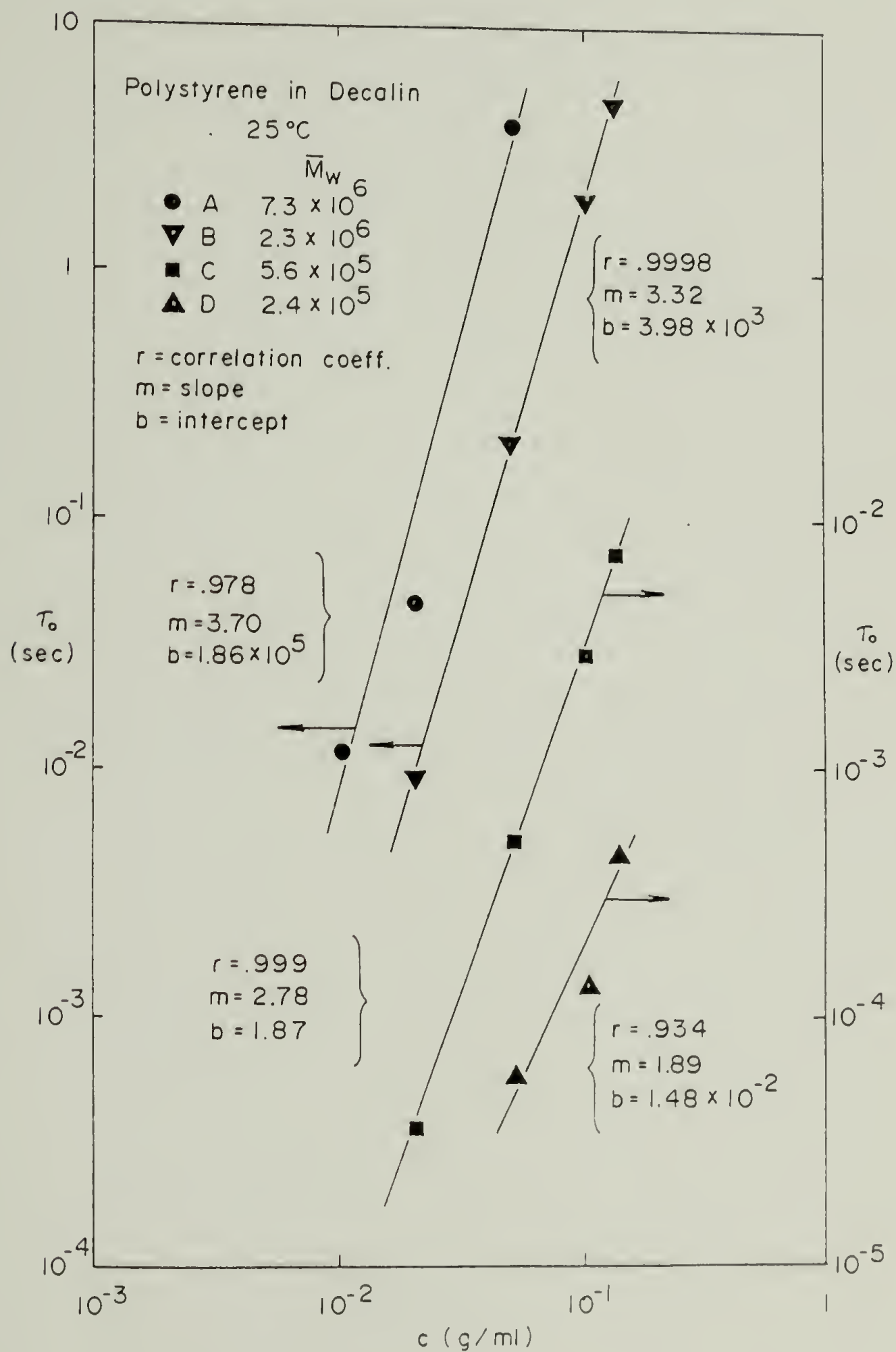Figure 13. Experimental Relaxation Time ($\log \tau_0$) versus Concentration ($\log C$) for Polystyrene Solutions

Figure 14. Ratio of Rouse Relaxation Time (τ_R) to Experimental Relaxation Time (τ_0) as a Function of Product of Concentration and Molecular Weight ($c\overline{M}_w$) for Polystyrene Solutions
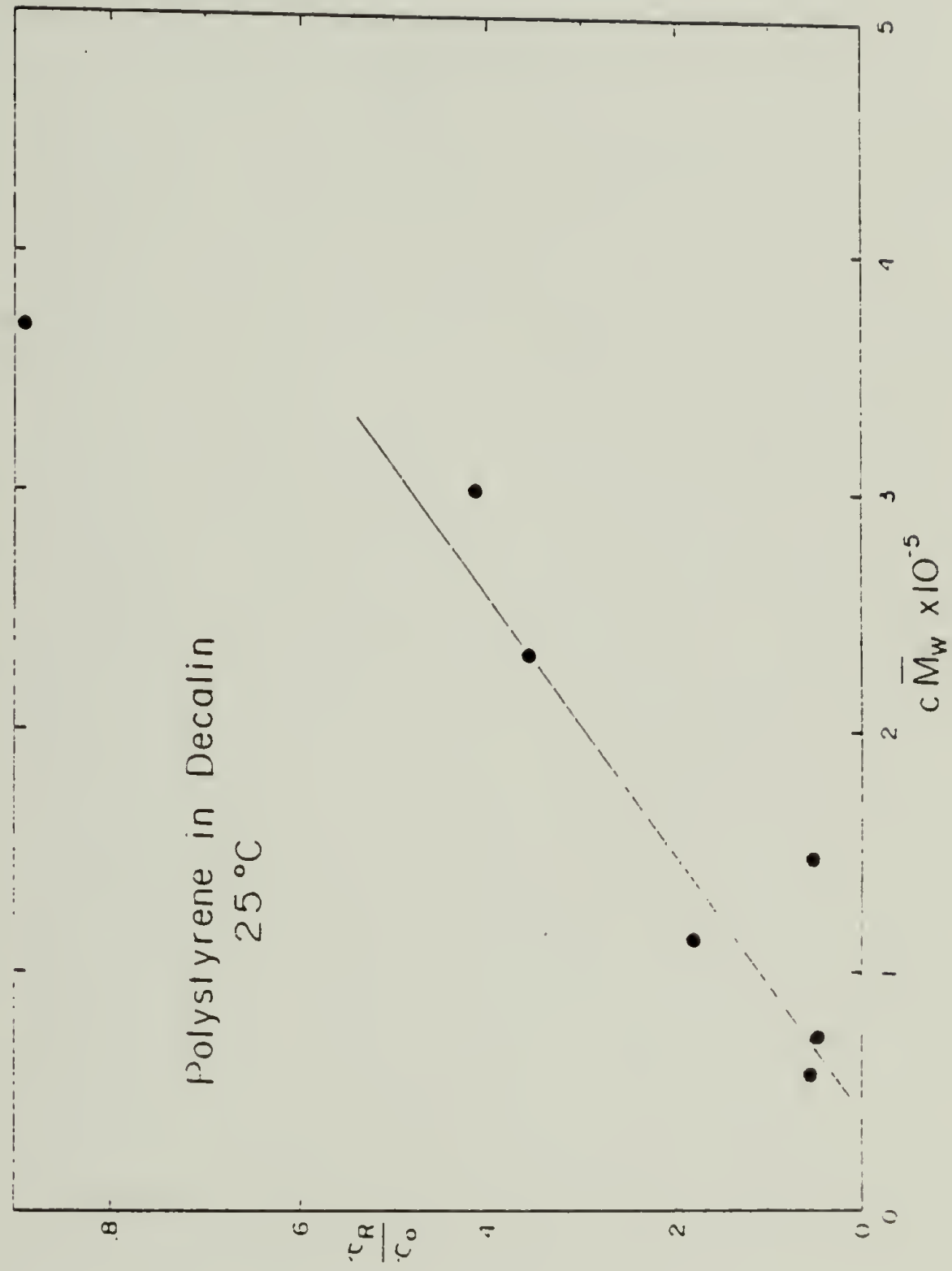
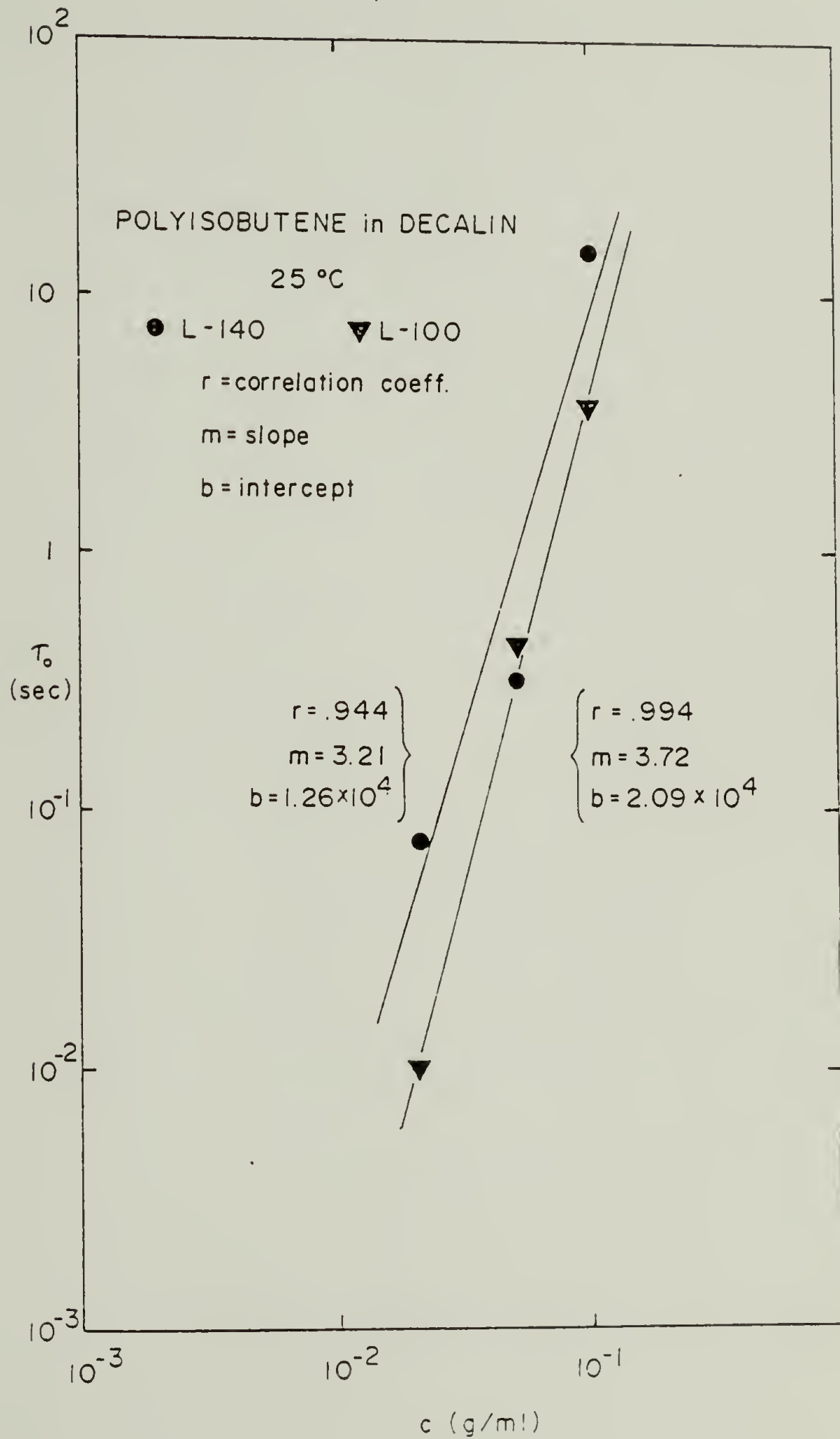Figure 15. Experimental Relaxation Time ($\log \tau_0$) versus Concentration ($\log$ C) for Polyisobutene Solutions
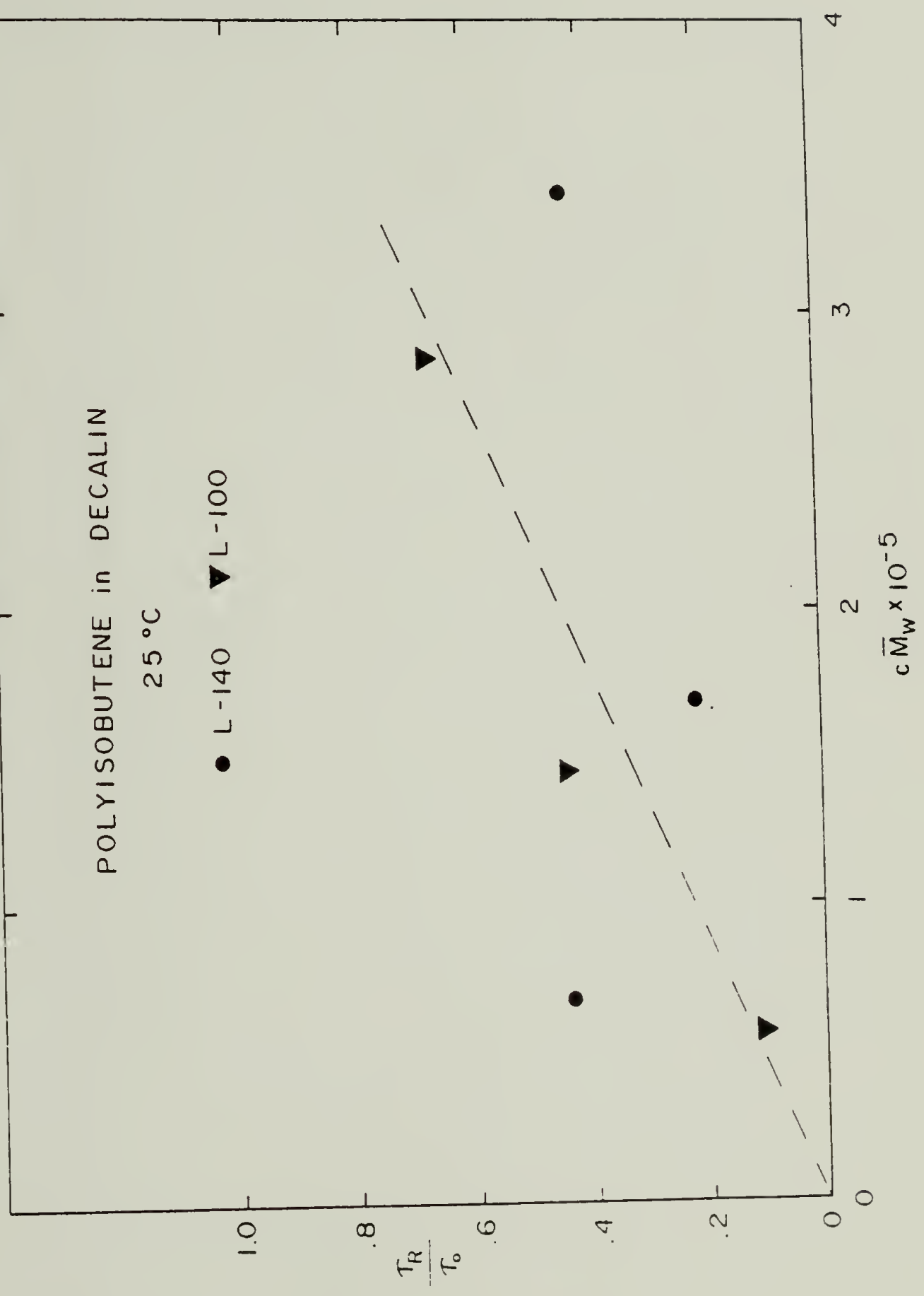
Figure 16. Ratio of Rouse Relaxation Time (τ_R) to Experimental Relaxation Time (τ_0) as a Function of Product of Concentration and Molecular Weight ($c\bar{M}_w$) for Polyisobutene Solutions

V.4. References

1. W.W. Graessley, "Advances in Polymer Science", Vol. 16, Springer-Verlag, New York, 1974.

2. Y. Ito and S. Shishito, J. Polym. Sci., Polym. Phys. Ed., 11, 2283 (1973).

3. Y. Ito and S. Shishito, J. Polym. Sci., Polym. Phys. Ed., 12, 617 (1974).

4. A. Casale, R.S. Porter and J.F. Johnson, Rubber Chem. Tech., 44(2), 534 (1971).

5. E.M. Barber, J.R. Muenger and F.J. Villforth, Jr., Anal. Chem., 27, 425 (1955).

6. R.S. Porter, R.F. Klaver and J.F. Johnson, Rev. Sci. Instruments, 36, 1846 (1965).

7. L.A. Manrique, Jr., and R.S. Porter, Rheo. Acta, 14, 926 (1975).

8. L.A. Manrique, Jr., M.S. Thesis, 1972, University of Massachusetts.

9. R.B. Bird, R.C. Armstrong and O. Hassager, "Dynamics of Polymeric Liquids", Vol. 1, John Wiley, 1977.

10. Revised Manual of RMS-7200 Mechanical Spectrometer, Rheometrics, Inc., N.J., 1977.

11. K. Walters, "Rheometry", Halsted Press, New York, 1973.

12. Z. Grubisic, P. Rempp and H. Benoit, J. Polym. Sci., B(5), 753 (1967).

13. Robert Jenkins, unpublished results.

14. K.B. Abbas and R.S. Porter, J. Appl. Polym. Sci., 20, 1289 (1976).

15. Manual of Model 200 Gel Permeation Chromatography, Waters Associates, Inc., Mass., 1974.

16. J.D. Culter, K.G. Mayhan, G.K. Patterson, A.A. Sarmasti and J.L. Zakin, J. Appl. Polym. Sci., 16, 3381 (1972).

17.   K. Arisawa and R.S. Porter, J. Appl. Polym. Sci., $\underline{14}$, 879 (1970).

18.   K.B. Abbas, T. Kirschner and R.S. Porter, accepted, Europ. Polym. J.

19.   R.S. Porter and J.F. Johnson, J. Appl. Phys., $\underline{35}$, 3149 (1964).

20.   W.W. Graessley, J. Chem. Phys., $\underline{47}$, 1942 (1967).

21.   R.A. Stratton, J. Colloid Interf. Sci., $\underline{22}$, 517 (1966).

22.   W.W. Graessley, R.L. Hazelton and L.R. Lindeman, Trans. Soc. Rheo., $\underline{11(3)}$, 267 (1967).

23.   M.F. Johnson, W.W. Evans, I. Jordan and J.D. Ferry, J. Colloid Sci., $\underline{7}$, 498 (1952).

24.   E.L. Slagowski, L.J. Fetters and D. McIntyre, Macromolecules, $\underline{7}$, 394 (1974).

25.   Y. Kato, T. Kametani and T. Hashimoto, J. Polym. Sci., Polym. Phys. Ed., $\underline{14}$, 2105 (1976).

26.   A. Casale and R.S. Porter, "Polymer Stress Reactions", Academic Press, New York, 1978.

27.   N.K. Baramboin, Polym. Sci., U.S.S.R. (Eng.), $\underline{4}$, 41 (1973).

28.   F. Bueche, J. Appl. Polym. Sci., $\underline{4}$, 101 (1960).

29.   K.W. Scott, J. Polym. Sci., $\underline{C(46)}$, 321 (1974).

30.   J. Brandrupt and E.H. Immergut, Ed.), "Polymer Handbook", Wiley-Interscience, 1975.

31.   A. Ram and A. Kadim, J. Appl. Polym. Sci., $\underline{14}$, 2145 (1970).

32.   R.E. Harrington and B.H. Zimm, J. Phys. Chem., $\underline{69}$, 161 (1965).

33.   R.S. Porter, M.J.R. Cantow and J.F. Johnson, J. Polym. Sci., $\underline{C(6)}$, 1 (1967).

34.   A.H. Abdel-Alim and A.E. Hamielec, J. Appl. Polym. Sci., $\underline{17}$, 3769 (1973).

35.   G.C. Berry and T.G. Fox, "Advances in Polymer Science", Vol. 5, Springer-Verlag, New York, 1968, p. 267.

36. R.S. Porter and J.F. Johnson, J. Polym. Sci., 50, 379 (1961).

37. R.N. Shroff and M. Shida, J. Polym. Sci., A(2)-8, 1917 (1970).

38. K. Kirschke and H. Mewes, "Proc. 5th. Int'l. Cong. Rheology", S. Onogi (Ed.), Vol. 1, University of Maryland Press, 1969, pp. 517-528.

39. Y. Ito and S. Shishito, J. Polym. Sci., Polym. Phys. Ed., 13, 35 (1975).

40. Y. Ito and S. Shishito, J. Polym. Sci., Polym. Phys. Ed., 16, 725 (1978).

41. A.F. Talbot, Rheo. Acta, 13, 305 (1974).

42. M.C. Williams, A.I.Ch.E.J., 21, 1 (1975).

43. A. Casale, R.S. Porter and J.F. Johnson, Rev. Macro. Chem., 6, 387 (1971).

44. R.S. Porter and J.F. Johnson, Chem. Rev., 66, 1 (1966).

45. W.W. Graessley and L. Segal, Macromolecules, 2, 49 (1969).

46. W.W. Graessley and L. Segal, A.I.Ch.E.J., 16, 261 (1970).

47. W.F. Seyer and R.D. Walker, J. Am. Chem. Soc., 60, 2125 (1938).